UNIVERSITY OF OKLAHOMA

GRADUATE COLLEGE

QUANTIFICATION OF NANOPARTICLE INTERACTIONS WITH THE NANOPARTICLE CLEARANCE SYSTEM

A THESIS

SUBMITTED TO THE GRADUATE FACULTY

in partial fulfillment of the requirements for the

Degree of

MASTER OF SCIENCE

By

SKYLER QUINE

Norman, Oklahoma

2020

QUANTIFICATION OF NANOPARTICLE INTERACTIONS WITH THE NANOPARTICLE CLEARANCE SYSTEM

A THESIS APPROVED FOR THE

STEPHENSON SCHOOL OF BIOMEDICAL ENGINEERING

BY THE COMMITTEE CONSISTING OF

Dr. Stefan Wilhelm, Chair

Dr. Handan Acar

Dr. Marc Moore

Abstract

The goal of nanomedicine is to target therapeutic and diagnostic agents to target tissues. However, there are multiple physiological barriers which prevent nanoparticles from reaching the desired destination in the body. Progress has been made in rationally designing nanoparticles to evade physiological barriers and optimize biodistribution, but many still fail to demonstrate significant efficacy to attain clinical approval and use. Contributing to this problem is a lack of quantitative reporting and analysis of nanoparticle interactions with nanoparticle-clearing physiological compartments, which we call the Nanoparticle Clearance System (NCS). In this master's thesis, we quantify nanoparticle-NCS interactions through a literature review, a quantitative literature survey, preparation of liposomal nanoparticle formulations, and a planned experiment for future research. We identify certain promising techniques to evade the NCS such as the saturation strategy, and conclude that thorough quantitative reporting for novel nanoparticle formulations and the combination of nanomedicine with other fields of knowledge will lead to advances in the efficacy and safety of nanotherapeutics.

Table of Contents

1. Literature Review: Strategies for Overcoming Delivery Barriers in Nanomedicine

1.1 Literature Review Abstract

The premise of nanomedicine is to improve diagnosis and treatment by selectively targeting nanoparticles to diseased organs and cells. However, the targeting efficiency of current nanomedicines is limited due to delivery barriers inside the body that sequester the majority of administered nanoparticles before reaching targeted tissues. Such delivery barriers include the organs and cells of the body's nanoparticle clearance system (NCS). Here, we explore and discuss NCS biology and mechanisms of action at organ and cellular levels. We review strategies that have been developed to mitigate nanoparticle-NCS interactions. These strategies can be divided into two general categories: (1) nanoparticle design strategies to evade the NCS, and (2) biological modulation strategies which reduce nanoparticle NCS interactions. We also report findings from a literature survey of the effects of these strategies on biodistribution. Although our findings show that the interactions of nanoparticles with the NCS can be difficult to predict, greater understanding of NCS function will provide design strategies for next generation nanomedicines with improved diagnostic and therapeutic performance by overcoming delivery barriers in the body.

1.2. Introduction

Nanoparticles can be used in medicine as therapeutic and diagnostic agents due to their uniquely tunable physicochemical properties, including size, shape, surface chemistry, and material composition, and their capacity for loading with drugs and contrast agents. However, the efficient delivery of nanoparticles to diseased tissues and cells in the body is a key challenge in nanomedicine. For example, a recent meta-analysis of preclinical studies found that only 0.7% (median) of systemically administered nanoparticles reach solid tumor tissues.[1] In addition, up to 99% of systemically administered nanoparticles may end up in the liver (Figure 1.1A).[2] These delivery challenges may contribute to the limited clinical translation of cancer nanomedicines.[3,4]

Efficient and effective nanoparticle delivery is a complex challenge because, upon entering the body, nanoparticles face numerous barriers. These challenges are posed by the physiological chemical and molecular environment,[5,6] the tumor or target cells,[7–9] and the cells and organs of the nanoparticle clearance system (NCS). In this review, we focus on the NCS barrier, which includes cell-mediated mechanisms such as opsonization, cell uptake through endocytosis,[10] direct translocation,[11,12] and neutrophil extracellular traps (NETs),[13] and cell-independent mechanisms such as filtering by the kidneys. NCS clearance often starts with nanoparticle-protein interactions in the blood (Figure 1.1B) which may lead to nanoparticle uptake by NCS cells (Figure 1.1C). The NCS barrier is part of the human body's own immune system: cells such as mononuclear phagocytes, leukocytes, and endothelial cells located in tissues throughout the body engulf nanoparticles by various uptake mechanisms. This segment of the immune system is often described in the literature as Mononuclear Phagocyte System (MPS) or Reticuloendothelial System (RES). These terms are sometimes used indiscriminately. To overcome the NCS barrier,

two main strategies have been developed: (i) the modulation of nanoparticle design, and (ii) the modulation or pre-treatment of the body's biological environment.

In this review, we explore the recent strategies and methods for improving nanoparticle pharmacokinetics and biodistribution. We characterize and summarize nanoparticle-NCS interactions by clarifying MPS/RES terminology and suggesting the broader NCS term, defining the mechanistic roles of NCS organs and cell populations in nanoparticle uptake, and describing the two distinct paradigms (i.e. modulation of nanoparticle design and modulation of the biological environment) which researchers have used to help nanoparticles evade the NCS. We further survey the literature to explore the effects on biodistribution of certain nanoparticle design and biological modulation strategies, synthesizing this information into key insights for the field of nanomedicine.

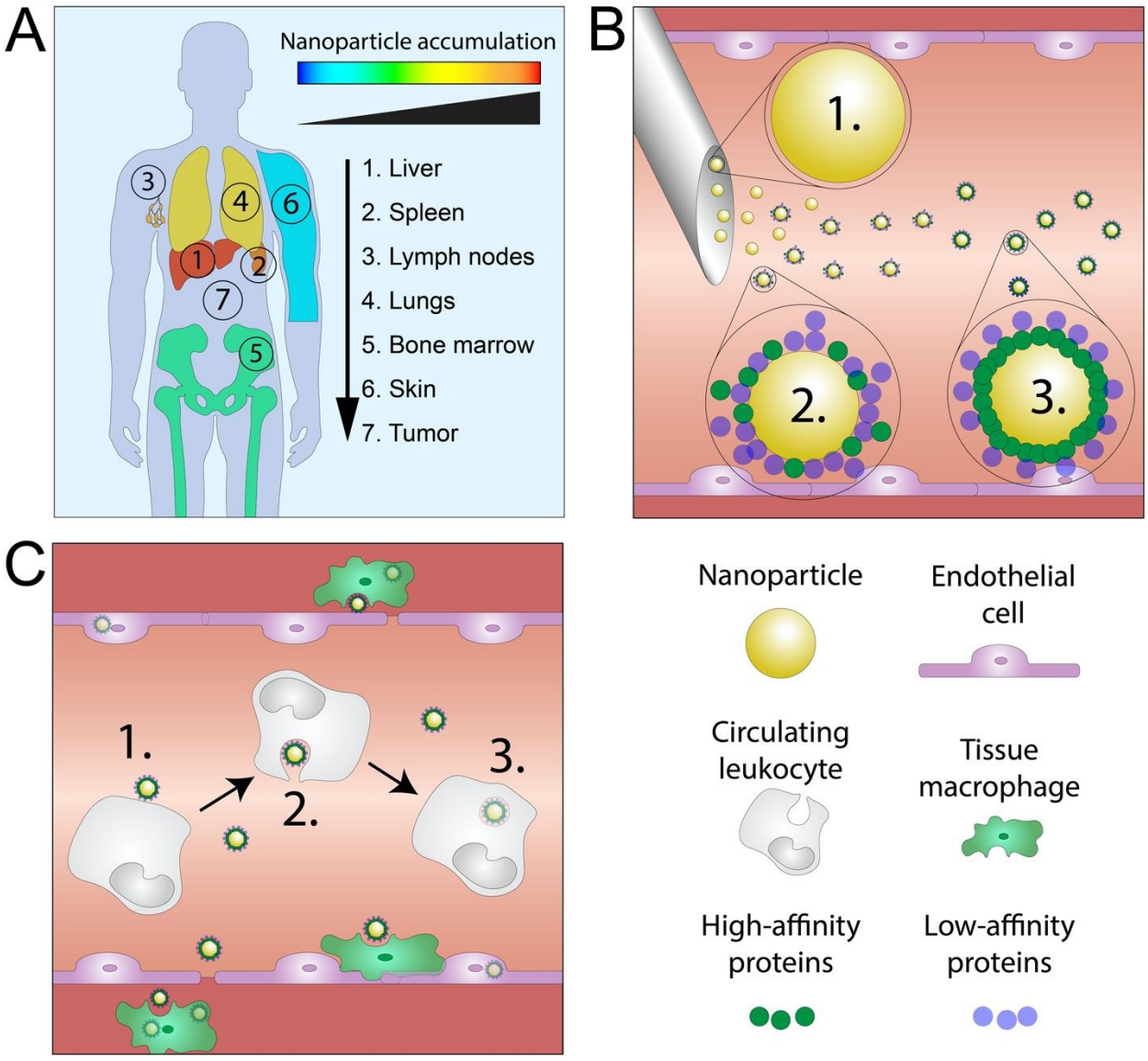

Figure 1.1: Examples of nanoparticle delivery barriers. (A) The body's biological and physical barriers affect nanoparticle biodistribution. Note: Depicted relative biodistribution may vary significantly for different nanoparticle formulations and doses. (B) Upon intravenous administration (1), nanoparticles are exposed to blood components. This exposure changes the nanoparticle synthetic identity to a biological identity (2). Proteins with varying binding affinities interact dynamically with the nanoparticle surface, forming a soft protein corona. Over time (3), a hard protein corona forms around the nanoparticle surface composed of proteins with relatively

high binding affinity. Proteins with less affinity interact with the hard corona and form a dynamic soft corona. (C) Cells of the nanoparticle clearance system (NCS), including tissue-resident macrophages, circulating leukocytes, and various endothelial cell types, uptake nanoparticles by a variety of mechanisms.

1.3. Mononuclear Phagocyte System, Reticuloendothelial System, and Nanoparticle Clearance System

The MPS and RES are both terms used to categorize cells and organs which pose biological barriers to nanoparticles through endocytosis and other mechanisms. Although both MPS and RES are relevant for nanoparticle sequestration and uptake, their use in the literature is inconsistent.[14–19] The term 'RES' was first used to describe any cell which accumulated systemically administered vital stains (dyes which can be used to stain living tissues), which at the time were thought to be endothelial in nature.[20] The term 'MPS' was introduced as a replacement when it was discovered that many of the cells involved in clearing macromolecules and foreign particulates from the blood were actually from monocyte and bone marrow origin.[21,22] However, subsequent research observed true endothelial cell types actively clearing material from the blood,[23] including scavenger endothelial cells (SECs)[24] such as liver sinusoidal endothelial cells (LSECs).[18,25,26] Therefore, the MPS and RES can be conceptualized as two separate systems which participate in sequestration of foreign material mediated by two different classes of cells. The MPS categorizes under the term 'mononuclear phagocyte' three ontologically and functionally distinct cell types which endocytose nanoparticles: monocytes, macrophages, and dendritic cells (DC's).[27,28] The RES comprises various endothelial cell types which exhibit endocytic behaviors.

Yet, MPS and RES categories leave out certain cell types, including leukocytes such as B cells and T-cells, which are capable of internalizing nanoparticles.[29,30] Further, RES and MPS systems rely on endocytic nanoparticle sequestration mechanisms, leaving out physical mechanisms such as glomerular filtration. We suggest 'nanoparticle clearance systems' (NCS) as a more practical and general term to describe organs, cells, and other mechanisms which are important in clearing nanoparticles from the blood and mediating elimination from the body. Cell-mediated NCSs include the MPS, RES, and other cellular mechanisms of nanoparticle sequestration and clearance. Cell-independent NCSs include physical mechanisms such as glomerular filtration in the kidneys and the unique flow profile of the liver (see section 3.2).

1.4. Nanoparticle Clearance System Organs

Cell-mediated NCS mechanisms

When a nanoparticle enters the body, it transitions from its lab-designed 'synthetic identity' to its physiologically-influenced 'biological identity' (Figure 1.1). Plasma proteins form what is known as a 'protein corona' around the nanoparticle, blocking its interactions with target cells and increasing non-specific interactions. Inclusion of opsonins in the protein corona can mark a nanoparticle for phagocytosis by circulating leukocytes or tissue-resident macrophages.[31] This can occur through the alternative, classical, and lectin pathways of the complement cascade, a bloodborne sector of the immune system which protects the body from foreign pathogens and particles.[32–34] Nanoparticle uptake can also occur through other types of endocytosis, including clathrin-dependent endocytosis, caveolae-mediated endocytosis, clathrin and caveolin independent endocytosis, and macropinocytosis. The various mechanisms for cellular

internalization of nanoparticles are reviewed in greater detail by Donahue et. al.[35] These cell-mediated NCS mechanisms occur in almost all NCS organs in a variety of cell types.

Cell-independent NCS mechanisms

Cell-independent mechanisms take on unique forms in different organs. For example, the glomerular filtration process in the kidneys is quite distinct from the flow profile and structure of the liver sinusoid. There is often an interplay between the cell-independent and cell-mediated mechanisms of an NCS organ, and they combine to control that organ's overall interactions with nanoparticles. In this section, we summarize current research on nanoparticle sequestration mechanisms in different NCS organs.

1.4.1. Blood

When nanoparticles enter the bloodstream, they are immediately faced with a complex biological environment.[36,37] Nanoparticles may interact with any blood component: biomolecules such as serum proteins, sugars, and lipids, and cells including red blood cells, white blood cells, and endothelial cells.[38–40] All of these interactions are highly dependent on nanoparticle design. Nanoparticles have been reported to interact with red blood cells in different ways: (i) lyse red blood cells (hemolysis),[41] (ii) passively enter them,[42] and (iii) adsorb to the RBC membrane for transport.[43] Besides mediating protein corona formation and opsonization, which promotes uptake in other NCS organs, the blood can function as its own NCS 'organ' by sequestering nanoparticles into various circulating cells. A study by Yang et. al. reported a time-dependent distribution of 500-nm polystyrene nanoparticles in blood cells. Nanoparticle uptake by granulocytes peaked at three hours, uptake by B cells peaked at six hours, uptake by monocytes peaked at twelve hours,

and uptake by phagocytic double negative ($B220^{-}CD11b^{+}Gr\text{-}1^{-}Ly\text{-}6C^{-}$) cells, 74% of which were CD11c+ dendritic cells, emerged at twelve hours and increased until 96 hours. The results suggested that granulocytes were responsible for most nanoparticle uptake in the blood and that the nanoparticles induced the differentiation of monocytes into dendritic cells and macrophages, increasing their presence in the blood.[44] Although these uptake characteristics are likely different for other nanoparticle formulations, the findings of Yang et. al. highlight the complexity of nanoparticle-blood interactions and warrant analysis of blood uptake patterns for novel nanoparticle formulations.

1.4.2. Liver

It has been reported that between 30 and 99 percent of an administered dose of nanoparticles is sequestered by the liver.[2] This high level of uptake is made possible by the large portion of cardiac output received by the liver (25%), the large numbers of macrophages found in the liver, and the liver's micro-architecture.[45–47] The architecture of the liver is shown in Figure 1.2, and has a marked effect on the liver's uptake ability. Stellate cells and the arterial buffer response regulate vasodilation in the liver,[48] resulting in 1000 fold slower flow in the sinusoids than in systemic circulation and increased probability of nanoparticle-cell interactions.[45] Nanoparticle uptake is generally greater close to the portal triad, and Kupffer cells have been shown to take up the highest number of hard nanoparticles, followed by B cells, then endothelial cells, then T cells and other cell types.[45]

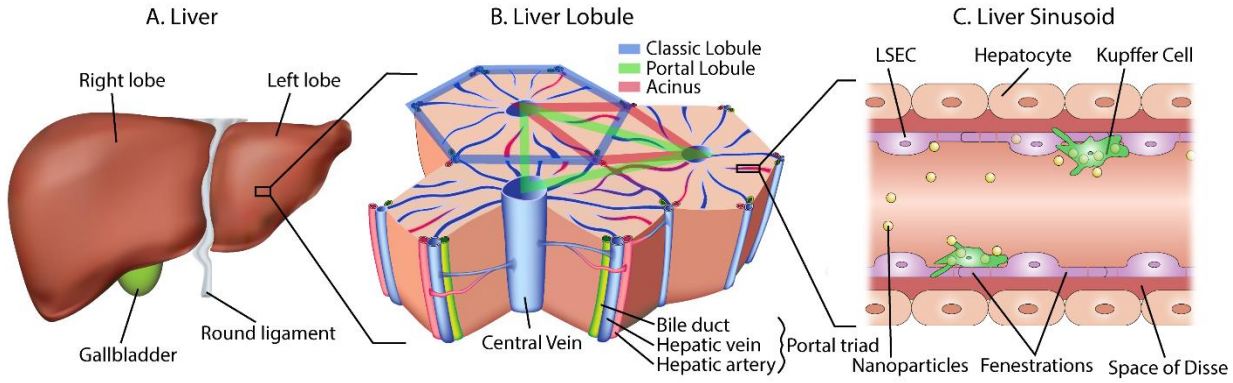

Figure 1.2: Schematic of liver architecture. (A) The liver is composed almost homogeneously of microscopic functional units called liver lobules (B). Blood flows into the liver via the hepatic veins and arteries. These two vessels, together with the bile duct, form the portal triad. Blood flows from each portal triad to the three nearest central veins, and bile flows in the opposite direction to collect in the bile duct for excretion. The classic lobule model is composed of a hexagon tracing the six nearest portal triads surrounding a given central vein. The portal lobule model is visualized with a triangle connecting three adjacent central veins. The acinus model is described as a diamond shape with two portal triads on the short axis and two central veins on the long axis. The acinus model is most relevant to nanoparticle clearance, as it emphasizes blood flow from the portal triads and the vessel network connecting them to the central vein. As blood flows towards the central vein, it passes through small vessels called sinusoids (C). Blood velocity decreases significantly, and the blood is allowed to interact with various cell types. As shown in panel (C), nanoparticles in the blood interact with different cell types, including Kupffer cells (macrophages), fenestrated liver sinusoidal endothelial cells (LSECs), and hepatocytes. The liver sinusoids are the primary location in the body where clearance of foreign material from the blood occurs.

1.4.3. Spleen

Weighing an average of 150g, the spleen is approximately 0.2% of human body weight but receives 5% of cardiac output.[49] As shown in Figure 1.3B, the spleen is divided into two main compartments: the red pulp and the white pulp. The white pulp contains macrophages, lymphocytes, dendritic cells, and plasma cells, but its function is primarily related to the antigenic immune system. The red pulp contains macrophages, reticular cells, lymphocytes, hematopoietic cells, plasma cells, and plasmablasts, and is primarily tasked with the removal of foreign material and aged red blood cells from systemic circulation. The red pulp macrophages are the most numerous resident macrophages of the spleen. Dendritic cells and two distinct types macrophages in the marginal zone also have the ability to phagocytize pathogens and foreign material.[50]

Red pulp macrophages and marginal zone macrophages and dendritic cells in the marginal zone actively phagocytize foreign material, including nanoparticles, passing through the arterioles and sinusoids of the spleen.[51,52] The nanoparticle distribution within the spleen can also heavily depend on model species and nanoparticle characteristics.[53] Nanoparticle accumulation in the spleen is assisted by the filter-like characteristics of the splenic sinusoids (Figure 1.3C), resulting in much higher uptake levels for nanoparticles over 200 nm in diameter.[54] Particles hindered by the small slits in the splenic sinusoids can be subsequently taken up by various splenic cells. However, recent studies have begun to overcome the variety of splenic barriers and found that soft, zwitterionic nanoparticles are able to deform and pass between slits in the venous sinusoids of the spleen, passing back into circulation and avoiding splenic entrapment and macrophage clearance.[55] When large particles (e.g., 500 nm polystyrene particles) are trapped in the spleen, they are

predominantly taken up by B cells. Dendritic cells are also highly involved, followed by a high number of macrophages (relative to blood and bone marrow), monocytes, and granulocytes.[44]

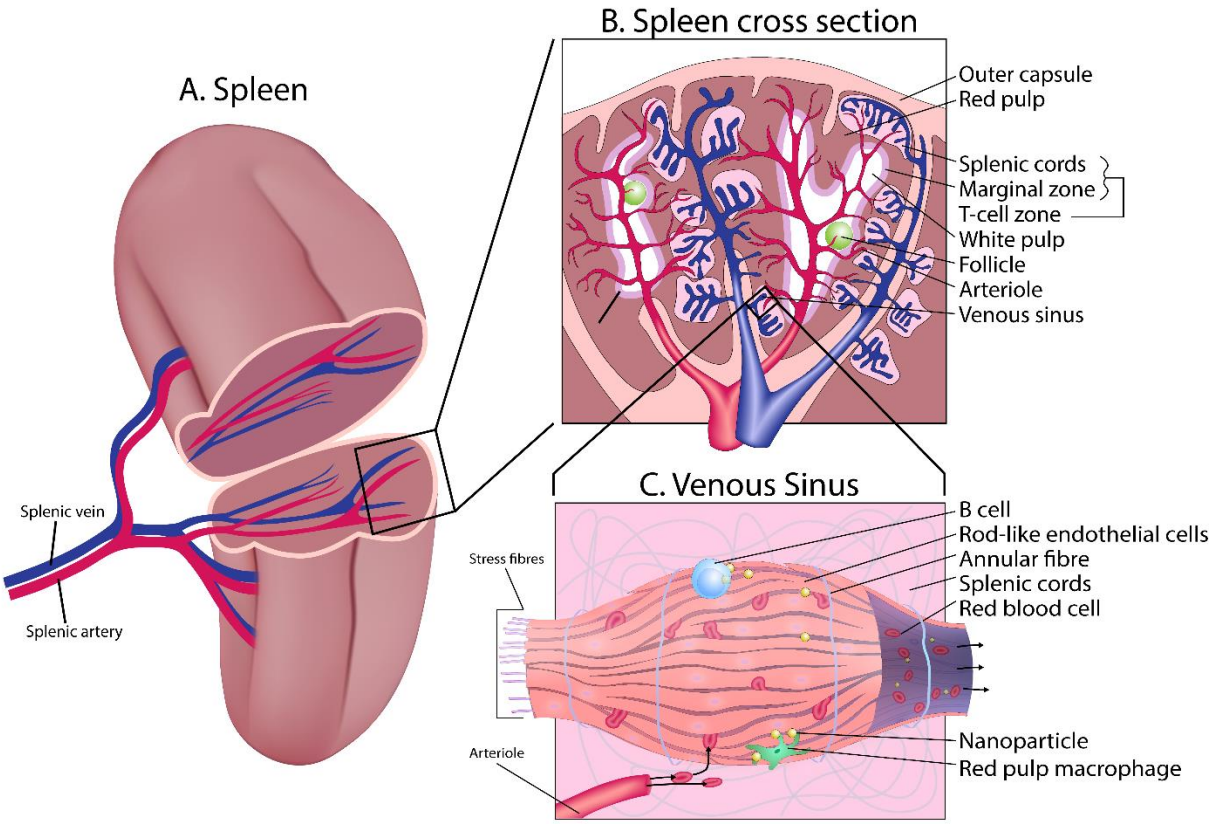

Figure 1.3: Schematic of spleen architecture. (A). The spleen is fed by arterial blood through the splenic artery and drains through the splenic vein. Arterial blood flows through arterioles and out into the white and red pulp of the spleen. (B). A small amount of blood is processed in the white pulp, and the complex lymphoid (adaptive immunity) function of the spleen is carried out. The majority of blood flows out of the branched arterioles into the red pulp of the spleen. The blood is pushed into the splenic cords and collects in the splenic sinuses to exit the spleen. (C). The splenic sinuses are composed of unique, lengthened endothelial cells with parallel stress fibers and perpendicular annular fibers contributing to its filtering function. Slits in the sinuses allow healthy RBCs to pass through, while old or damaged RBCs with less flexible membranes are excluded and persist in the cords until they are phagocytized by red pulp macrophages. This size

exclusion mechanism can hinder re-entry of large nanoparticles into the bloodstream, which are subsequently taken up by B cells, macrophages, and dendritic cells.

1.4.4. Lungs

The lungs receive 100% of cardiac output. They also receive venous blood from every tissue in the body, which undergoes gas exchange in the alveolae.[56] The three main types of macrophages in the lungs are alveolar macrophages, pleural macrophages, and pulmonary intravascular macrophages (PIMs).[57] For intravenously administered nanoparticles, PIMs are the main concern since they are in contact with blood in the capillaries of the lung.[58] However, the populations of PIMs in the lungs are poorly defined in humans. Other cell types, such as endothelial cells and neutrophils, are likely also involved in the processing and surveillance of venous blood. Interactions of various cell types in the lungs with foreign material from venous blood is not well described in literature.[59] Few studies currently exist which analyze the distribution of venously administered nanoparticles in physiological compartments of the lung or among cell types. The majority of literature focuses on inhaled nanoparticles, in which alveolar macrophages play a large role, mediated by surfactant protein A, which enhances nanoparticle uptake when part of the protein corona.[60,61]

1.4.5 Bone Marrow

The bone marrow is the primary hematopoietic organ and is also a primary lymphoid tissue, producing RBCs, various types of WBCs, and platelets. It is located in the core of bones throughout the body.[62] To supply the body with the cells it produces, it receives a significant blood flow through feeding arteries, which then drains through venous sinuses and exits the bone through

nutrient veins.[63] The marrow sinusoidal system is different from that of the spleen and liver in that it comprises a thin, flat layer of endothelial cells between the bone and marrow.[64] These endothelial cells are called marrow sinusoidal endothelial cells (MSECs), and demonstrate significant endocytic behavior of particulate matter, including nanoparticles.[65] This function is related to that of the splenic SECs and red pulp macrophages, as the bone marrow is similarly tasked with the removal of old or damaged RBCs from circulation.[66] The bone marrow has been reported to uptake as much as 50% ID of nanoparticle formulations in some cases, but this degree of uptake occurs primarily with smaller particles which have evaded the liver and spleen through polymer surface modification.[67] With larger (500 nm) polystyrene nanoparticles, Yang et. al. demonstrated prolonged (>96 hours) residence of nanoparticle in the bone marrow, with granulocytes dominating nanoparticle uptake. In contrast to blood-mediated nanoparticle uptake in the same study, bone marrow uptake among cell populations did not fluctuate as much with time, and double negative (Gr-1^{neg}, Ly6C^{neg}, mostly dendritic) cells were the most efficient population in phagocytizing nanoparticles.[44] Another study showed that CD11b+ Gr-1+ cells are recruited by polymeric nanoparticles (PLGA/OVA) in the bone marrow, and that these cells can then cross-present the nanoparticle-borne antigen, resulting in antigen-specific T cell proliferationan.[68]

1.4.6. Skin

The skin is the largest vascularized organ of the body and carries out multiple functions including protection, sensing, and maintenance of homeostasis.[69] Some biodistribution studies mention accumulation in the skin, usually reporting minimal accumulation in comparison to other organs.[70–72] However, these studies do not mention the cells involved or mechanism of uptake in the skin. A unique study by Sykes et. al described accumulation of gold nanoparticles and quantum

dots in the skin in greater detail. This study found that nanoparticles accumulate in in the skin in quantities linearly correlated with administered dose. More specifically, nanoparticles were found in DCs and dermal macrophages with low administered doses, while they distributed more generally in the pericellular space of the dermis and subcutaneous tissue at higher doses.[73] The higher accumulation of nanoparticles in non-macrophage cell populations at higher doses could be due to saturation mechanisms of phagocytic cells. Further, nanoparticles were cleared from the skin over time and drained into the lymphatic system and lymph nodes. Thus, nanoparticle accumulation in the skin and lymphatic system is closely related.[73]

1.4.7. Lymph Nodes

The lymph nodes are integral in the functioning of both adaptive and innate immunity, antigen processing, and mounting defenses against a host of foreign pathogens. They contain three types of macrophages: subcapsular sinus macrophages, medullary sinus macrophages, and medullary cord macrophages.[74] Yang et. al show that major populations involved in polymeric nanoparticle uptake in lymph nodes include B cells, dendritic cells, monocytes, and granulocytes, although lymph node accumulation at six hours was found to be significantly lower than in other organs.[44] Larger nanoparticles (50-100nm) are retained for long periods of time (>5 weeks) in the follicles, while smaller ones (5-15nm) are quickly cleared in under 48 hours.[75] In addition to nanoparticle size, lymph node accumulation is also very dependent on time: at later time points (12 h), lymph node uptake of nanoparticles has been reported to outstrip even liver distribution.[76] It has been suggested that lymph node accumulation may increase over time because the lymphatic system drains nanoparticle-containing DCs from other tissues such as the skin.[73] However,

nanoparticles can also get to lymph nodes apart from DC-mediated transportation: nanoparticles are often transported to lymph nodes as extracellular particles in the lymph.[76]

1.4.8. Kidneys

Finally, it is worth noting that the kidneys are not included in the NCS organs list because their predominant mechanism of clearing nanoparticles from the blood depends on physical glomerular filtration rather than uptake by resident immune or endothelial cells. It is widely accepted that nanoparticles with diameters less than approximately six nanometers will be quickly cleared from circulation by the kidneys.[77] However, the kidneys can also be induced to promote the clearance of larger nanoparticles through incorporation of a glycan surface modification.[78] For interested readers, nanoparticle-kidney interactions are reviewed in greater detail by Du et. al.[79]

1.4.9. Tumor

Due to large populations of immune cells in some tumors such as tumor-infiltrating myeloid cells (TIMCs) and tumor associated macrophages (TAMs), tumors can be viewed as another NCS organ.[80] Usually, this is seen as a barrier to nanoparticle delivery to tumors. Often, nanoparticles are taken up by TAMs instead of cancer cells,[81] a fact that is not always represented well when nanoparticle accumulation in a whole tumor is imaged by fluorescence or quantified by digesting the entire tumor for elemental analysis. Yet rather than presenting an insurmountable problem, the uptake of nanoparticles by TAMs represents an opportunity to target these tumor-associated immune cell populations for immunomodulary cancer therapies. It has been suggested that there are at least ten subtypes of macrophages, four subtypes of monocytes, four subtypes of dendritic cells, five subtypes of neutrophils, and two subtypes of mast cells present in the tumor

microenvironment. They are variously associated with good or bad cancer outcomes, presenting a host of potential targets for stimulation, suppression, repolarization, and other immunomodulary strategies.[80] Various reviews have described this immune-targeting strategy since at least 1988, and the idea warrants further development and research.[82,83]

1.5. Nanoparticle design strategies

1.5.1. Intrinsic Design

Nanoparticle design can be categorized into (i) intrinsic design, which refers to a nanoparticle's physical and chemical characteristics, and (ii) surface design, which refers to surface modifications added to the nanoparticle surface which can mediate its interaction with the physiological environment. One of the ways to control nanoparticle interactions with the NCS is by changing nanoparticle physical and chemical characteristics. There are many different properties which affect the nanoparticle's interaction with the NCS,[84] but they fall under the main categories of material, size, shape, and surface charge. The effects of these physicochemical properties on NCS-nanoparticle interactions have been well studied, and certain combinations of desirable characteristics promise to make future nanomedicines more efficient and effective. However, despite extensive research on effect of physicochemical properties on cell uptake, nanoparticle-cell interactions continue to defy generalizations due to the complexity of mechanisms at play and lack of standardization of models, procedures, and nanoparticles themselves.[85]

1.5.1.1. Material

A wide range of materials are used to make nanoparticles and nanomedicines, including metals like gold, silver, and iron oxide, polymers like poly-lactic acid (PLA) and poly(lactic-co-glycolic acid) (PLGA), and biomolecules such as lipids, albumin, and dendrimers. Because nanoparticles are usually decorated with surface molecules, the specific interactions of material type with serum proteins and NCS cells are difficult to characterize *in vivo*. Despite this difficulty, the effect of nanoparticle composition on cell interactions has been reported in some studies. For example, an increased cholesterol content in liposomes has been linked to generation of reactive oxygen species and apoptosis in macrophages.[86] However, the main effects of nanoparticle material on cellular interactions and biodistribution have to do with the material's influence on physical characteristics such as nanoparticle elasticity and porosity.

Elasticity

The elasticity of nanoparticles is commonly quantified by Young's Modulus, which is expressed in Pascals and measures a material's deformation in response to applied pressure.[87] High elasticity is associated with harder or stiffer materials, and low elasticity with softer and more flexible ones. In order to study the effect of nanoparticle elasticity on cellular interactions and biodistribution, various types of nanoparticles with tunable elasticity have been designed. The main types of tunable elastic nanoparticles include hydrogel nanoparticles, hybrid polymer-lipid nanoparticles, and silica nanocapsules.[88] Nanoparticle elasticity can influence biodistribution by modulating interactions with NCS cells and NCS organ filtration processes.[89]

Numerous studies have described interactions of nanoparticles of varying elasticity with multiple cell lines, but results are often conflicting. For example, less elastic liposomal

nanoparticles are able to fuse with cell membranes, leading to decreased endocytosis times for lower elasticities.[90] However, for (polymer core)-(lipid shell) nanoparticles, a lower elasticity led to increased cellular internalization times.[91] This demonstrates the importance of material when considering the effect of elasticity on direct cell interactions. Shen et. al. reported that membrane wrapping efficiency may be a function of both receptor diffusion and kinetic driving force, meaning that cell internalization time potentially depends on nanoparticle shape and cell type.[92] The complexity of interacting factors (nanoparticle material, nanoparticle shape, and cell type) between studies may account for the variation in results.

Nanoparticle elasticity does not only affect interactions with NCS cells, but also interactions with NCS organ macrostructures. Especially salient are nanoparticle interactions with the spleen. As a result of the filter-like microstructure previously described, less elastic nanoparticles can deform and squeeze through the slits between the endothelial cells of the splenic sinus, much like healthy RBCs.[93] However, the longer circulation time that results does not necessarily translate to higher tumor or target organ accumulation: since in some cases soft nanoparticles see reduced internalization in NCS cells, they can resist uptake by tumor or target cells in the same way that they resist NCS endocytosis.

1.5.1.2. Nanoparticle Size

A key determinant of the biological fate, toxicity, and health effects of nanoparticles is their size.[94–96] Nanoparticle size is often measured using dynamic light scattering and confirmed with physical imaging methods such as TEM, and the values found in literature usually report the hydrodynamic diameter in aqueous solution.[97] Due to the complex interactions between

nanoparticle properties and study models, it is difficult to establish consistent and exact biodistribution patterns based only on size.[98] However, some general rules can be summarized which can be used to inform nanoparticle design. Small nanoparticles (<6 nm) are quickly cleared from the body by the kidneys. Such small nanoparticles can also see a greater retention in vascular endothelium.[99] The effects of larger sizes on interactions with the various NCS organs are less definitive. Generally, nanoparticles of all sizes greater than 6 nm tend to accumulate predominantly in the liver and spleen. In the 6-100 nm size range, smaller nanoparticles tend to distribute more equally into multiple organs, while larger ones tend to have a higher percentage concentration in the liver and spleen.[100,101] Based on the physical filtering characteristic of the splenic sinusoids, nanoparticles with >200 nm diameter would be expected to have increased splenic distribution. Splenic distribution has been shown to increase with sizes up to ~200 nm,[102] but some studies report a decrease in splenic accumulation with even larger sizes.[103] This could be due to increased nanoparticle uptake by the lungs, liver, and other NCS organs before reaching the spleen, since very large particles see increased distribution in those organs.[2] The differing dynamics between sizes of nanoparticles can be attributed in part to the effect of nanoparticle size on protein corona formation.[104] Overall, 1-6 nm nanoparticles are quickly cleared by the kidneys or are retained in vascular endothelium, 6-150 nm nanoparticles experience higher accumulation in the liver and spleen with increasing diameter, ~200nm nanoparticles distribute in greater quantities to the spleen relative to other sizes, and <250 nm nanoparticles tend to experience efficient hepatic and sometimes lung clearance. A challenge with the modulation of nanoparticle size is that larger nanoparticle size can inhibit deep penetration into tumor tissues.

1.5.1.3. Nanoparticle Shape

The geometric structure of a nanoparticle can also direct its biodistribution. Despite a focus on spherical nanoparticles in many studies and clinical applications, a diverse body of literature suggests that non-spherical shapes consistently exhibit longer circulation times and lower degrees of phagocytosis by NCS cells. The reason for longer circulation times for non-spherical nanoparticles is two-fold: less energetically favorable cellular interaction, and improved vascular margination dynamics. The efficiency of endocytosis of nanoparticles on a cellular level is highly dependent on shape. Even for just ellipsoid nanoparticles, oblate and prolate geometries have different internalization and attachment kinetics.[105] Shape can have a large effect on whether a nanoparticle comes into contact with macrophages at all. Nanorods, nanoworms, filomicelles, and nanodisks all exhibit hydrodynamic behavior markedly different from spherical nanoparticles. Specifically, filamentous, string-like nanoparticles such as nanoworms and filomiclles may orient themselves in the direction of blood flow and distribute mainly in the center of flow, decreasing interactions with any NCS cells on the vascular walls or in sinusoids.[106] Because of greater circulation time due to optimal positioning within blood flow, non-spherical nanoparticles of various types accumulate less in the liver and spleen, and more in the more vascularized organs of the NCS. However, this trend can be somewhat unpredictable since even small changes in geometry can greatly affect a nanoparticle's biodistribution. For example, short nanorods have demonstrated higher accumulation in the liver, in contrast to higher splenic accumulation for long nanorods.[107] This underscores the need for precision and intentionality in nanoparticle design and engineering.

1.5.1.4. Charge

Another factor affecting the uptake and biodistribution of nanoparticles is their surface charge, usually measured by zeta potential.[108] Generally, nanoparticles with neutral surface charge (-10 mV to 10 mV) have longer circulation times and slower accumulation in the NCS than nanoparticles with large negative or positive charges (< -10 mV or >10 mV).[77,109] Levchenko et. al showed that liposomes with a more neutral charge exhibited slower clearance from the blood than negatively charged liposomes (~ -40 mV), which accumulated in the liver.[110] Another study on liposomes reported that positively charged liposomes quickly aggregated with serum proteins, which promoted a change to negative charge and subsequent sequestration by the NCS.[111] A study involving gold nanoparticles found that positive or negatively charged nanoparticles tend to locate in the red pulp of the spleen and the hepatocytes and endothelial cells of the liver, while nanoparticles with neutral charge tend to accumulate in the white pulp and Kupffer cells.[112] Based on these findings, it is possible that nanoparticles with greater positive and negative charges have more non-specific cellular interactions while nanoparticles with neutral charge initially circulate longer before accumulating more opsonins and being taken up to a relatively greater extent by professional phagocytes. Further, nanoparticle charge has an effect on the uptake mechanism by various cell types. With some exceptions, positive nanoparticles generally use a wide variety of mechanisms, while negatively charged nanoparticles are more likely to use caveolae mediated endocytosis.[113] However, the exact effects of nanoparticle charge on uptake mechanism are difficult to generalize and contradict between studies (See Table 3). Surface charge is commonly modulated by the addition of charged moieties to the nanoparticle surface; some of these moieties are discussed in the following section.

1.5.2. Surface Modification

The external design of nanoparticles plays a major role in directing interactions with the NCS.[10] The surface conjugants of nanoparticles, from simple polymers to biologically-inspired ligands and membrane structures, determine the fate of the nanoparticle by influencing the composition of the protein corona and interacting with specific biological entities.[35,114] The ability to easily undergo specific surface modification is a primary draw for the development and use of nanoparticles for therapy and drug delivery. Various surface modifications of nanoparticles can be categorized by their mechanism of action. Some surface modifications such as PEG and other synthetic polymers rely entirely on steric inhibitions to decrease interactions with serum proteins and cells. Other surface modifications rely on biologically inspired inhibitions, such as the use of carefully selected ligands to intentionally inhibit interactions with specific circulatory and cellular components. As shown in Figure 1.4, most nanoparticle surface modifications fall somewhere between these two paradigms, since almost any ligand which is selected to inhibit a specific NCS component will also demonstrate some steric-inhibitory function.

One of the oldest and most common SM methods for minimizing interactions of nanoparticles with biological systems is PEGylation.[115] PEGylation involves conjugating poly-ethylene-glycol to the surface of a nanoparticle via chemical methods.[116] PEGylation prevents the interaction of the nanoparticles with the biological environment through steric inhibition and formation of an aqueous layer around the nanoparticle due to its hydrophilic nature.[117] In order to prevent PEG from covering nanoparticle targeting moieties, a method called PEG backfilling can be used.[118] Additionally, it has been suggested that the optimum MW of PEG to minimize macrophage recognition is 2000 Da.[119] PEGylation has been widely researched and is known to increase the circulation times of numerous nanodrug formulations, [120,121] but new research points

to problems that may limit its effectiveness in clinical applications.[122] Some humans have already developed anti-PEG antibodies, and after one treatment of a PEGylated therapy, further treatments are cleared more quickly – a phenomenon called the accelerated blood clearance effect (ABC).[123] PEGylated nanoparticles can also be endocytosed through various pathways, as PEGylation only delays formation of a protein corona and eventual sequestration by the NCS.[124] A mechanism by which cysteine, followed by serum proteins, replace PEG and destabilize the nanoparticle, has been proposed, and this problem can be partially circumvented through the incorporation of a hydrophobic layer between the nanoparticle and hydrophilic PEG layer.[125] This hydrophobic shield solution, however, does not solve the ABC problem. A huge variety of other polymers have been synthesized which have a similar mechanism of action to PEG, such as polaxamers, polaxamines, and polysaccharides.[115] Generally, these methods of surface modification are united in their mechanism, which relies on modulating nanoparticle surface hydrophobicity: hydrophilic surface modification promotes the formation of a layer of hydration around the nanoparticle, minimizing nonspecific interactions with other components in solution. Hydrophobicity has been shown to have a strong effect on corona formation and macrophage uptake, which is a reason why it remains a popular choice for minimizing nanoparticle-NCS interactions.[126]

Proteins and other molecules can be conjugated to nanoparticle surfaces using simple chemical processes similar to those used for PEGylation. An especially promising technique which relies strongly on a steric method of inhibition is the conjugation of zwitterionic ligands to the nanoparticle surface. These moieties consist of positively and negatively charged groups linked to a stem by a carbon chain, resulting in the overall presentation of a neutral charge.[127] A variety of studies have reported on the stability of these particles under physiological conditions, and their

stealth properties characterized so far demonstrate potential for more extensive exploration.[128–132] However, not all zwitterionic formulations are successful in evading the NCS system: one study found that a zwitterionic AuNP formulation accumulated extensively in the liver in spleen, even though it also had high tumor accumulation compared to other nanoparticles in the study.[133] Another technique, which utilizes the plasma protein serum albumin (a major component of nanoparticle protein coronas), can improve the pharmacokinetics of nanoparticles because the serum albumin forms the hard corona and competitively inhibits adherence of more biologically active serum components such as opsonins and antibodies.[134] A similar approach uses RNA complexes called aptamers to decorate the nanoparticle surface, protecting the nanoparticle from NCS sequestration and allowing for the targeting of specific biological niches.[135] Other techniques are even more biologically specific, coating nanoparticles with 'self-marker' proteins, normally recognized by macrophages and lymphocytes in order to avoid phagocytosis of healthy cells.[26] When these specific biological molecules are used, nanoparticles can be rendered invisible to the cell types that recognize those markers.[136] However, when only one specialized molecule or protein is used, the subset of cells avoided can be too specific and small. An approach that aims at less biological specificity is the encapsulation of nanoparticles in cell membranes, which already have a plethora of diverse self-peptides conjugated to their surface.[137] This approach has the greatest degree of biological inspiration, directly using a cell membrane as a trojan horse for nanoparticles to evade a wide variety of both specific and nonspecific NCS interactions.[138]

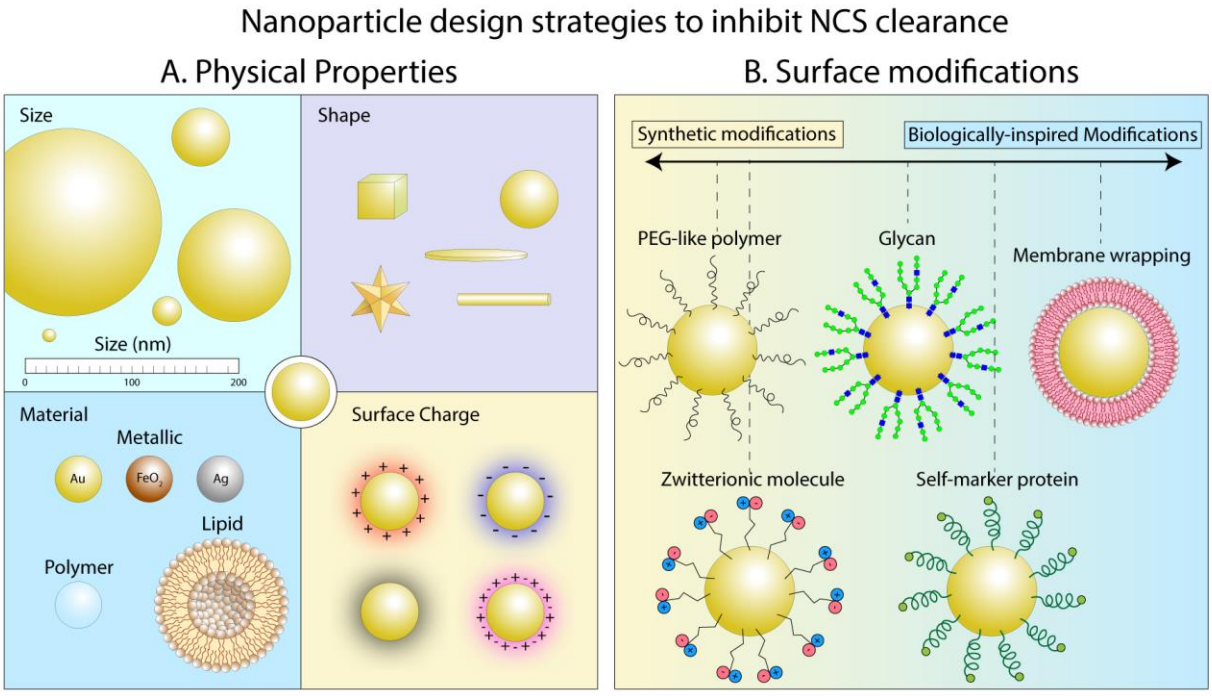

Figure 1.4: Nanoparticle design strategies to inhibit NCS clearance. (A) The intrinsic physical properties of nanoparticles can often be easily modulated to reduce uptake by NCS cells. Sizes of nanoparticles ranging from 3 nm to over 400 nm have been reported to affect nanoparticle biodistribution. Shape has a large effect on cell uptake due to modulation of intravenous flow profiles, protein corona characteristics, cell-nanoparticle contact surface area, and uptake mechanism. The material of a nanoparticle can influence the makeup of the protein corona. Finally, the surface charge of nanoparticle has been shown to change uptake profiles. Large positive or negative charges can increase sequestration probability while neutral and zwitterionic charge profiles reduce the chance of uptake. (B.) Nanoparticle surface modifications reported in literature are incredibly diverse. The designs can be divided into two categories: synthetic surface modification, which usually has a mechanism of steric inhibition, and biologically-inspired surface modification, which usually has a mechanism of biologically-targeted inhibition. Most surface

modifications exhibit some characteristics of both, falling somewhere in a continuous range between the two extremes. Here, examples are organized based on how much their design relies on synthetic modification (left of panel) and biologically-inspired modification (right of panel).

Table 1.2: Selected contradictions arising from complexity of nanoparticle-cell interactions

Primary finding	**Contradictory finding**
Increased size increases nanoparticle uptake efficiency[139–141]	Decreased size increases nanoparticle uptake efficiency[142]
Only nanoparticles with diameter <100nm enter cells through clathrin-dependent endocytosis[141,143]	Nanoparticles with diameter >100nm can enter cells through clathrin-dependent endocytosis[144–146]
Non-phagocytic cells do not endocytose nanoparticles >200nm[147]	Non-phagocytic cells endocytose nanoparticles >200nm[141,144]
Uptake is more efficient with positively charged nanoparticles[37,144–150]	Uptake is more efficient with negatively or neutrally charged particles[151–153]
Positively charged nanoparticles enter cells (at least partially) through clathrin-dependent endocytosis[10,149,150]	Positively charged nanoparticles enter cells through a mechanism other than clathrin-dependent endocytosis[153]
Opsonization of liposomes leads to increased cellular uptake[154–157] *	Opsonization of liposomes leads to decreased cellular uptake[158–160] *
Zwitterionic surface modification prevents NCS uptake[128–132] *	NCS uptake of zwitterionic surface modified nanoparticles is comparable to other formulations[133] *
Low elasticity leads to less efficient cellular internalization[91] *	Low elasticity leads to more efficient cellular internalization[90] *
Splenic accumulation increases with increase in nanoparticle size up to ~200nm[102] *	Splenic accumulation decreases with increase in nanoparticle size[103] *
Targeted surface modifications increase tumor accumulation *	Targeted surface modifications decrease tumor accumulation[161] *

There are a great number of variables at play in nanoparticle-cell interactions. The nanoparticles themselves are often different between studies, with changes in composition, charge, size, and surface modification. Further, immune and non-immune cells in the body use a variety of

endocytic mechanisms to uptake nanoparticles, and mechanisms may differ even for small changes in nanoparticle formulation. Finally, a lack of standardization in both *in vitro* and *in vivo* models contributes to the difficulty of generalizing any patterns relating nanoparticle design to interactions with the body. Adapted and expanded from Table 1, Interactions at the cell membrane and pathways of internalization of nano-sized materials for nanomedicine. Valentina Francia, Daphne Montizaan et. al. Beilstein Journal of Nanotechnology, 11, 1, 2 2020. Contributions from this review are denoted with *.

1.6. Biological environment modulation strategy

The biological modification strategies currently described in literature can be divided into three primary categories, depicted in Figure 1.5: (1) the saturation of NCS cells with blank nanoparticles so they cannot uptake subsequently administered nanotherapeutics, (2) the use of drugs to inhibit and endocytic mechanisms of NCS cells, and (3) the use of drugs to directly kill tissue macrophage populations.

1.6.1. Saturation strategies

Although over the NCS is capable of processing multiple doses of nanoparticles over a long period of time,[162] it has a limited short-term capacity which is naturally limited by the amount and rate of foreign material each cell is able to internalize. One study by T. Liu et al. showed that overloading the NCS with blank liposomes could increase tumor accumulation of iron nanoparticles two-fold.[163] This strategy could represent a way to increase nanoparticle circulation time with a relatively low-toxicity pretreatment, and warrants further development and study.[164]

1.6.2. Inhibition strategies

Various drugs have been shown to inhibit the phagocytic mechanisms of the NCS. These include chloroquine, gadolinium chloride, and methyl palmitate.[165–167] Chloroquine and gadolinium chloride work by inhibiting the phagocytic mechanisms of macrophages.[166] Wolfram et al. chose chloroquine as an ideal candidate from among other known phagocytic inhibitors and demonstrated a decrease of accumulation in the liver by 28.5% for liposomes and 22% for discoidal silicon nanoparticles.[168] Similarly, Deorukhkar et al. used gadolinium chloride to mitigate accumulation of quantum dots in the NCS and increase their usefulness as an imaging agent for tumors.[169]

1.6.3. Suicide strategies

Other drugs have been used to deplete tissue macrophage populations. One drug commonly used for this purpose is clodronate. The technique of using clodronate liposomes to deplete liver macrophages was first developed by van Rooijen et al.[170,171] Hao et al used clodronate liposomes to deplete liver macrophages and improve the biodistribution of PTX PLGA nanoparticles. Macrophage populations subsequently recovered and little to know toxic side effects were observed during the study.[172] Chan et al. showed that pretreatment with clodronate liposomes was an effective way to decrease the uptake of nanoparticles by kupffer cells in the liver.[173] This technique has been used in other studies to decrease nanoparticle accumulation in the liver, increase circulation time, and increase tumor accumulation of intravenously administered nanoparticles.[174–177]

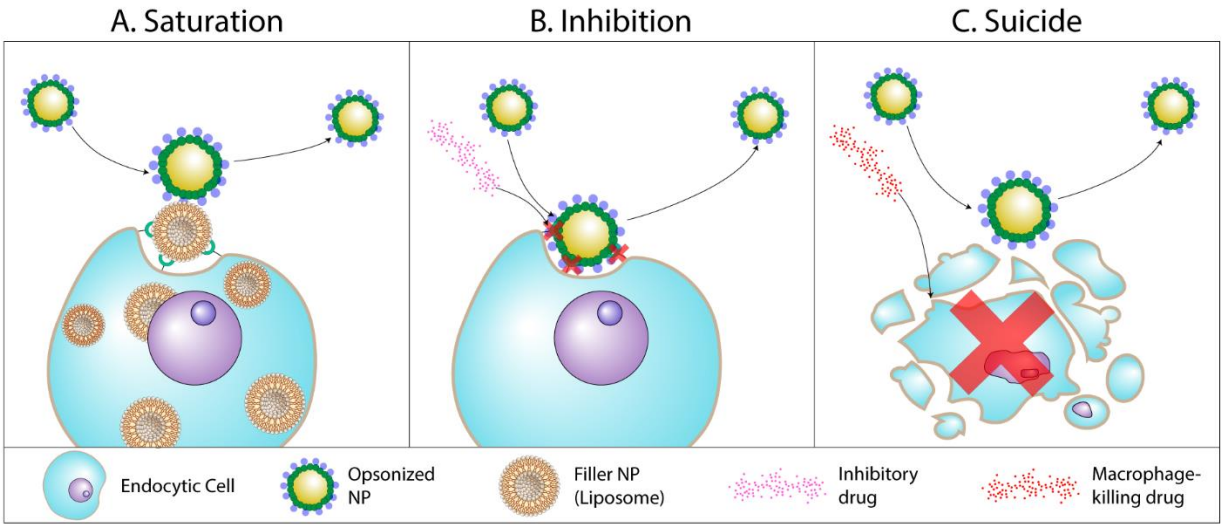

Figure 1.5: NCS preconditioning strategies. (A) Saturation preconditioning strategies work by overloading NCS cells with a non-therapeutic nanoparticle. The nanoparticle used for saturation is usually chosen to be nontoxic and should degrade easily after a period of time. Because NCS cells are full of the saturating nanoparticle and their uptake rates are saturated, they cannot further phagocytize more nanoparticles, allowing subsequently and/or simultaneously administered therapeutic nanoparticles to evade the NCS and distribute more effectively to target tissues. (B) Inhibition strategies make use of drugs which block interactions of NCS cells and nanoparticles. One mechanism is the disruption of endocytosis mechanisms by blocking receptor-nanoparticle corona interactions. nanoparticles escape attachment to NCS cell membranes and are free to interact with target tissues. (C) In the macrophage suicide strategy, chemicals are used to induce apoptosis in all or part of resident tissue macrophage populations. Because the NCS cells are dead, they cannot sequester nanoparticles.

1.7. Literature Survey

1.7.1. Method

In order to further characterize the interactions of NCS organs and nanoparticle design or biological preconditioning strategies, a survey of nanoparticle biodistribution studies was conducted. Papers were sought by searching Google Scholar for the keywords "nanoparticle biodistribution." In order to be selected for the survey, a biodistribution study had to be conducted on at least two different nanoparticle formulations or at least one biological modification strategy with a non-modified nanoparticle control. A candidate study had to display biodistribution data from at least two of the analyzed organs (liver, spleen, blood, tumor, heart, lung, and skin) in a measurable manner. When possible, data was gathered directly from numbers or tables in the literature. When only a graph or chart was reported, ImageJ was used to manually measure the height of bars or points, and actual values were calculated from the pixel values using the y-axis scale of the graph. An Excel spreadsheet was used to analyze and store the data, all of which has been made available in the Supplementary Information. Data was analyzed by calculating the percent change in biodistribution for each organ related to a change in formulation. For example, if accumulation in the liver of a range of four nanoparticle sizes was reported in the literature, the nanoparticle accumulation in the liver for the larger three would be compared to the accumulation in the liver for the smallest. These changes in biodistribution were represented in percent change from the original formula or control calculated using Equation 1:

Equation 1: ((Changed Formulation – Original Formulation)/Original Formulation)*100

In this way, whether data was reported as %ID/organ, %ID/g, total fluorescence, or any other paradigm, the relevance of comparing effects of formulation changes on biodistribution changes between papers is maximized.

1.7.2. Results

When a nanoparticle is injected into the body, it must go somewhere. If it resides longer in the blood, it will accumulate less in other compartments. If it accumulates in the liver, it will be present in other compartments to a lesser extent. If it passes by the liver, accumulation in the other NCS compartments, and hopefully the tumor, will be greater. This is the basic logic behind the development of many NCS-evasion strategies. Some studies analyzed supported this hypothesis, with negative percent changes in the liver and spleen accompanied by positive percent changes in other organs, or vice versa. [111,163,169,178,179] Studies also supported this hypothesis when a positive percent change in the blood was accompanied by negative percent changes in other NCS compartments.[172] However, other studies showed less ordered or even counterintuitive patterns in biodistribution changes,[180–185] such as a nanoparticle formulation change leading to higher or lower accumulation in all organs measured, including the blood.[133] Even within a single study, data from one biodistribution quantification method (fluorescence imaging of whole organs) supported the NCS-evasion premise while data from quantification via flow cytometry had a less ordered biodistribution pattern.[102] However, as can be seen in Figure 1.6, there are some important exceptions. The various biological modification techniques consistently led to positive accumulation changes in the blood and negative accumulation changes in the liver. The changes in accumulation in the blood and liver resulting from changes in nanoparticle modulation strategies

were less consistent and showed a wide data spread. The variability of results from this survey suggest a few key conclusions.

First, as evidenced by multiple sections in this review, the interaction with and resulting biodistribution of nanoparticles in the immune system and organs of the body is convoluted and complex. Different nanoparticle formulations, different animal models, different species, different observation times, and different imaging and quantification paradigms yield diverse, sometimes opposite, conclusions. Even for nanoparticles of similar formulation, generalizations are difficult to make, emphasizing the importance of thorough biodistribution and toxicity studies for all novel nanoparticle formulations. New formulations must be treated on a case-by-case basis.

Second, it is imperative that biodistribution studies are thorough and represent as many relevant organs as possible. The importance of other organs and systems to nanoparticle function and toxicity has been made clear, and it is no longer sufficient to rely on pharmacokinetic data from only the liver, spleen, or blood. Data which depicts a lower distribution in all organs after a nanoparticle formulation change means that either the imaging method is faulty, a differing amount of nanoparticles was injected for each trial, some other error was made, or nanoparticles accumulated in a physiological compartment that was not analyzed. The goal of every biodistribution study should be to account for close to 100% of injected nanoparticle dose. If only certain organs are of interest, the remaining carcass should be digested and analyzed. Being thorough in this manner will either rule out or point to other errors in sample preparation, imaging methods, or injection errors like missing the tail vein. Nanoparticles cannot just disappear from an animal, so it is necessary to analyze their accumulation in the entire physiological system.

Third, quantitative methods of analysis should be used when possible. Fluorescent imaging can lead to different conclusions even within the same study,[102] and in other studies has been shown to be unpredictable and inconsistent for nanoparticle biodistribution analysis.[186] The results of quantitative analysis should be represented as %ID/g to emphasize relative interactivity of a cell population of interest and a nanoparticle, and also as %ID/organ to enhance relevance to biodistribution and possibilities for toxicity.

Table 1.3: Percent changes in biodistribution for different NCS-evasion strategies

Reference	Time	Strategy	NP	Liver	Spleen	Blood	Tumor	Heart	Lung	Skin
[163]	24h	Saturation	Targeted 3F-cy7.5	-0.298	-0.524	0.633	1.214	0.340	0.841	0.026
	24h	Saturation	Non-targeted 3F-cy7.5	-0.321	-0.452	0.571	0.428	0.270	0.492	0.143
	24h	Saturation	3F-DIR	-0.287	-0.379	0.417	0.583	0.737	0.567	0.125
[111]	10m	Saturation	DNA plasmid	-0.300					0.400	
[172]	6h	Suicide	PTX-PLGA	-0.658	-0.701	1.000		-0.111	-0.129	
[178]	15m	Inhibition	Discoidal silicon	-0.230	0.417	1.765		0.524	0.500	
	6h	Inhibition	Liposome	-0.304	0.023	0.721	0.920			
	6h	Suicide	Liposome	-0.639	1.294	1.333	0.680			
[169]	4h	Inhibition	EGF-QD	-0.475			0.629			
[187]	48h	RBC membrane	FA-RBC-UCNP	-0.350	-0.304	3.263	1.293	0.121	-0.287	
	48h	RBC membrane	RBC-UCNP	-0.261	-0.287	2.625	1.422	-0.135	-0.257	
[188]	24h	Size	50nm AuNP	-0.787	0.098	-0.500		-0.571	-0.701	
	24h	Size	100nm AuNP	-0.732	0.220	-1.000		0.714	-0.758	
	24h	Size	200nm AuNP	-0.638	0.707	-0.950		-0.143	-0.807	
[179]	3h	PEG	PEG-PLGA	-0.416	-0.069	9.000			0.496	
	6h	PEG	PEG-PLGA	-0.180	-0.063	15.909			0.696	
[189]	24h	Charge	-26.9mV	-0.422	-0.366		0.229		-0.427	
	24h	Charge	-17.5mV	-0.534	-0.298		0.536		-0.382	
	24h	Charge	-8.5mV	-0.592	-0.290		0.800		-0.438	
	24h	Charge	3.6mV	-0.548	-0.168		0.393		-0.281	
	24h	Charge	18.5mV	-0.427	-0.282		0.257		-0.169	
	24h	Charge	29.5mV	-0.230	0.122		0.157		-0.022	
[107]	2h	PEG	NSR	-0.147	-0.457	0.919			1.069	

	24h	PEG	NSR	0.073	-0.486	2.475			0.630	
	7d	PEG	NSR	0.776	2.583	0.548			1.818	
	2h	PEG	NLR	-0.381	-0.798	0.429			3.045	
	24h	PEG	NLR	0.056	0.035	-0.682			5.188	
	7d	PEG	NLR	0.636	1.875	-0.214			0.609	
	2h	Shape	NSR/NLR	-0.558	2.049	-0.505			0.138	
	24h	Shape	NSR/NLR	-0.018	-0.181	0.650			-0.652	
	7d	Shape	NSR/NLR	-0.421	-0.667	-0.333			0.045	
	2h	Shape	PEG-NSR/PEG-NLR	-0.679	0.136	-0.632			1.225	
	24h	Shape	PEG-NSR/PEG-NLR	-0.034	0.648	-0.849			0.320	
	7d	Shape	PEG-NSR/PEG-NLR	-0.467	-0.733	-0.662			-0.403	
[190]	1hr	PEG	Au-PEG750	-0.043		-0.713		-0.557	0.758	1.279
	24hr	PEG	Au-PEG750	-0.076		26.143		-0.214	0.386	1.059
	1hr	PEG	Au-PEG10k	-0.965		58.375		35.667	N/A	-0.879
	24hr	PEG	Au-PEG10k	-0.413		1284.714		9.000	3.429	-0.971
[184]	1d	Size	SiNP20/80	-0.685	-0.879	0.000		0.353	0.798	
	3d	Size	SiNP20/81	-0.643	-0.902	0.500		-0.563	0.110	
	5d	Size	SiNP20/82	-0.572	-0.867	0.000		-0.862	-0.674	
	15d	Size	SiNP20/83	-0.597	-0.810	0.000		-0.867	-0.751	
	30d	Size	SiNP20/84	-0.655	-0.853	0.000		-0.900	-0.841	
[191]	1hr	PEG	D/D5	-0.923	-0.538					
	1hr	PEG	D/D20	-0.909	-0.628					
[185]	72h	PEG/size	PLGA	1.164	0.900	0.050	3.625	ND	0.909	
	72h	PEG/size	PLGA	1.239	2.000	0.650	29.125	Large	6.364	
[183]	1hr	Size	DP/EP	0.477	0.362			0.000	0.291	
	4hr	Size	DP/EP	0.541	0.507			0.000	0.254	
	8hr	Size	DP/EP	0.250	0.288			0.000	0.329	
[192]	1d	Protein SM	MUA/citrate	-0.025	-0.687	0.110		0.750	0.389	
	1d	Protein SM	CALNN/citrate	-0.486	-1.082	0.748		0.750	0.264	
	1d	Protein SM	CALND/citrate	-0.337	-0.873	0.850		0.500	-0.222	
	1d	Protein SM	CALNS/citrate	-0.271	-0.403	0.701		0.750	0.278	
[182]	1d	Size	20nm/10nm Iron Oxide	0.896	0.420			0.102	0.179	
	1d	Size	30nm/10nm Iron Oxide	0.421	0.093			0.218	0.006	
	1d	Size	40nm/10nm Iron Oxide	0.549	-0.436			0.168	0.060	

	7d	Size	20nm/10nm Iron Oxide	0.238	0.261			-0.081	0.097
	7d	Size	30nm/10nm Iron Oxide	0.274	0.077			-0.185	-0.406
	7d	Size	40nm/10nm Iron Oxide	0.509	0.220			-0.050	-0.100
[181]	.5h	Size, material	PCL/PLGA	-0.009	1.908	-0.259			
	1hr	Size, material	PCL/PLGA	-0.248	2.720	-0.204			
	2h	Size, material	PCL/PLGA	-0.341	1.000	-0.312			
	4h	Size, material	PCL/PLGA	-0.406	1.528	-0.519			
	24h	Size, material	PCL/PLGA	-0.496	0.455	-0.672			
[180]	10m	PEG	PEG-SCKbac/SCKbac	-0.212	-0.188	1.529			0.750
	1hr	PEG	PEG-SCKbac/SCKbac	-0.201	-0.291	1.000			0.115
	4h	PEG	PEG-SCKbac/SCKbac	-0.318	-0.375	0.844			-0.568
	24h	PEG	PEG-SCKbac/SCKbac	-0.324	-0.558	0.500			-0.613
	10m	PEG	PEG-SCKsac/SCKsac	-0.164	-0.150	0.588			-0.451
	1hr	PEG	PEG-SCKsac/SCKsac	-0.178	-0.257	0.310			-0.235
	4h	PEG	PEG-SCKsac/SCKsac	-0.085	-0.261	0.243			-0.136
	24h	PEG	PEG-SCKsac/SCKsac	0.000	-0.173	0.349			0.000
	10m	PEG	PEG-SCKbsc/SCKbsc	-0.277	-0.726	-0.290			4.031
	1hr	PEG	PEG-SCKbsc/SCKbsc	-0.022	-0.503	-0.273			4.057
	4h	PEG	PEG-SCKbsc/SCKbsc	0.333	-0.300	-0.025			3.722
	24h	PEG	PEG-SCKbsc/SCKbsc	-0.021	-0.538	-0.051			4.000
	10m	PEG	PEG-SCKssc/SCKssc	0.169	-0.409	-0.139			-0.750
	1hr	PEG	PEG-SCKssc/SCKssc	0.128	-0.178	-0.136			-0.514
	4h	PEG	PEG-SCKssc/SCKssc	0.098	-0.351	0.211			0.000
	24h	PEG	PEG-SCKssc/SCKssc	-0.024	-0.220	0.574			-0.188
	10m	Size	SCKbac/SCKsac	-0.242	-0.657	0.000			-0.725
	1hr	Size	SCKbac/SCKsac	-0.220	-0.738	-0.103			-0.235
	4h	Size	SCKbac/SCKsac	-0.067	-0.664	-0.135			0.682
	24h	Size	SCKbac/SCKsac	0.271	-0.173	-0.209			1.214
	10m	Size	PEG-SCKbac/PEG-SCKsac	-0.286	-0.672	0.593			-0.125
	1hr	Size	PEG-SCKbac/PEG-SCKsac	-0.242	-0.750	0.368			0.115

	4h	Size	PEG-SCKbac/PEG-SCKsac	-0.305	-0.716	0.283			-0.158
	24h	Size	PEG-SCKbac/PEG-SCKsac	-0.140	-0.558	-0.121			-0.143
	10m	Size	SCKbsc/SCKssc	0.808	1.263	-0.900			0.714
	1hr	Size	SCKbsc/SCKssc	0.202	0.619	-0.860			0.892
	4h	Size	SCKbsc/SCKssc	-0.262	-0.099	-0.728			4.643
	24h	Size	SCKbsc/SCKssc	-0.232	-0.119	-0.426			1.813
	10m	Size	PEG-SCKbsc/PEG=SCKssc	0.119	0.049	-0.918			33.500
	1hr	Size	PEG-SCKbsc/PEG=SCKssc	0.042	-0.021	-0.882			18.667
	4h	Size	PEG-SCKbsc/PEG=SCKssc	-0.104	-0.028	-0.781			25.643
	24h	Size	PEG-SCKbsc/PEG=SCKssc	-0.230	-0.478	-0.654			16.308
	10m	Material	SCKbsc/SCKbac	0.244	2.875	-0.088			2.429
	1hr	Material	SCKbsc/SCKbac	0.228	2.473	0.269			1.692
	4h	Material	SCKbsc/SCKbac	-0.123	1.500	0.250			1.135
	24h	Material	SCKbsc/SCKbac	-0.294	0.209	0.147			0.452
	10m	Material	PEG-SCKbsc/PEG-SCKbac	0.142	0.308	-0.744			8.857
	1hr	Material	PEG-SCKbsc/PEG-SCKbac	0.503	1.436	-0.538			11.207
	4h	Material	PEG-SCKbsc/PEG-SCKbac	0.714	1.800	-0.339			22.313
	24h	Material	PEG-SCKbsc/PEG-SCKbac	0.022	0.263	-0.275			17.750
[133]	24h	Ligand	TTMA/TEGOH AuNP	-0.636	-0.383		-0.894		-0.639
	24h	Ligand	TCOOH/TEGOH AuNP	0.832	0.171		-0.404		4.059
	24h	Ligand	Tzwit/TEGOH AuNP	0.846	-0.174		-0.028		2.234
[102]	24h	Size	166nm PLGA/120nm PLGA	0.246	2.024			-0.224	-0.216
	24h	Size	283nm PLGA/120nm PLGA	0.593	3.512			-0.276	-0.427
	24h	Size	443nm PLGA/120nm PLGA	0.547	3.146			-0.586	-0.643
	24h	Size	166nm PLGA/120nm PLGA	-0.175	1.456			-0.556	-0.872
	24h	Size	283nm PLGA/120nm PLGA	-0.456	0.684			-0.778	-0.915
	24h	Size	443nm PLGA/120nm PLGA	1.965	1.386			-0.583	-0.938

1.8. Discussion

While nanoparticles designed to better evade the immune system may help improve pharmacokinetics for certain applications, they face a few key challenges. First, biological barriers to efficient drug delivery through nanoparticles are complex and very diverse. They comprise a large range of organs and cell types and have evolved specifically to keep foreign matter like nanoparticles out of systemic circulation. If a nanoparticle gets past the liver, it has a multitude of other organs to evade. If it is designed to evade phagocytosis, it can be engulfed by a number of other endocytic mechanisms displayed by a host of non-immune cells such as scavenger epithelial cells. If it evades cellular uptake, it can be sequestered by physical filtering methods of the kidneys and splenic sinusoids. The complexity and thoroughness of our body's defenses are astounding, and even with years of development and refinement in nanoparticle design, recent reviews have concluded "we are not quite there yet."[193]

Another challenge is the gap in current research on nanoparticles and their interactions with the body. Papers detailing new nanoparticle formulations often focus primarily on new and improved targeting strategies, and their biodistribution studies are limited and incomplete. While more efficient targeting is a large need in the field, formulation studies must also consider biological interactions in order to be clinically relevant. More comprehensive biodistribution studies (quantifying accumulation in all organs and cell types of interest) for emerging nano-formulations will be key in understanding the interactions of different materials, properties, and surface functionalities of nanoparticles with the organs and cell types in the body. With this information, a nanoparticle design library can be created to inform clinical decisions and selection

candidates for specific disease paradigms. Further, nanoparticles can be engineered more easily and intentionally with a clear understanding of biological interactions.

A third challenge is the lack of bioinert nanoparticle formulations. While a truly bioinert nanoparticle may not be feasible, new surface modifications or cloaking strategies are needed to give nanoparticles the circulation time they need to distribute into their target tissue. PEG may be outliving its heyday as research continually points to its inadequacy. This is especially relevant in certain cancer applications, as tumor accumulation is sometimes correlated to circulation time. Conversely, approaches that safely and temporarily incapacitate the NCS to render it 'blind' to nanoparticles warrant further development and comprehensive testing. Many studies already demonstrate encouraging results, and these may be combined with other strategies for synergistic effect. Other challenges include inconsistent analysis and reporting methods for nanoparticle biodistribution, lack of whole-animal consideration in biodistribution reporting, and inconsistent data presentation approaches.

1.9. Future Directions

One solution to the challenges summarized above is to carry nanoparticle design as far as technology will take it, increasing specific interactions with target cell populations and decreasing nonspecific interactions wherever possible. This sounds simple, but as seen in this review, the challenge is incredible. Even if a 100% bioinert nanoparticle could be developed, it would avoid target cell populations in the same way that it avoids non-target populations, since the assumption of passive targeting through the EPR effect is being replaced by greater knowledge of cell-

mediated transport mechanisms.[194] Whenever targeting moieties are added, there is some potential for non-specific interaction no matter how specific the ligands are. Nanoparticles may end up in the tumor microenvironment due to prolonged circulation, but they may not interact with tumor cells. The pursuit of increasingly bioinert formulations, then, may be logically self-defeating. However, the solution of pursuing better nanoparticle designs is not without merit. In the example of Doxil, increased toxicity to tumors and survival of patient populations is marginal, but systemic toxicity due to the chemotherapeutic drug is markedly reduced.[195,196] This pattern is also seen in other current formulations.[197] Therefore, although nanoparticle-delivered toxic drugs may not demonstrate increased efficacy over free-administered formulations, they have great potential to increase safety profiles. Further, great progress has been made in predicting and selectively avoiding NCS uptake, especially in the liver and spleen, suggesting the possibility that the efficacy and safety of nanoparticle formulations has a future for improvement.[198]

Another solution to the challenges listed above is to stop trying to avoid seemingly unavoidable immune interactions and use them instead. Many new nanotherapies are currently being developed, and a new field combining nanomedicine and immunotherapy has emerged. The immune interactions of nanoparticles have even been reported to improve prognosis of acute pathologies such as brain injury.[199] Other studies focus on targeting the lymph nodes for immunomodulary applications.[200,201] More exciting studies involving cancer therapies in this developing field are wonderfully reviewed by Darrel J. Irvine and Eric L. Dane.[202] Further, the favorable accumulation of nanoparticles in specific NCS organs can be leveraged; for example, lipid nanoparticles can be used to deliver nucleic acids to liver hepatocytes for the potential treatment of hepatic pathologies.[203] Many other NCS organs are associated with specific and widespread pathologies, as in the case of lung cancer and liver cancer. These pathologies represent

an opportunity to use the strengths and tendencies of nanoparticle biodistribution patterns instead of fighting them.

1.10. Conclusion

In this review, we first explored the macro and micro-structure of organs and cells important in the capture of nanoparticles from systemic circulation. Consideration and knowledge of these interactions will lead to greater understanding of the challenges nanomedicine faces and the ultimate advance and development of the field. Understanding the function of these organs and the cells within them is essential for designing strategies to minimize their interactions with nanoparticles. We then looked at strategies which have been developed to overcome biological barriers to nano-delivery. The first group of these strategies are all based on modulating characteristics of the nanoparticle itself. Key strategies include modulating nanoparticle size, shape, or charge, steric inhibition SM strategies such as PEGylation, biologically inspired SM strategies such as the attachment of self-marker ligands, and bio-mimetic strategies including membrane cloaking. The second group of these strategies focus on modulating the biological environment of the NCS. Key strategies include the depletion of tissue-resident macrophages with toxins such as chlodronate, the inhibition of phagocytic pathways with drugs such as chloroquine, and the saturation of NCS cells by overloading them with blank and non-toxic nanoparticles. A literature survey reported the effects of some of these strategies on nanoparticle biodistribution patterns. Even though the results of this analysis were diverse and sometimes counterintuitive, they point to key opportunities for improvement in the field of nanomedicine. Specifically, more quantitative analytical methods, better consistency and accuracy in biodistribution reporting methods, thorough investigation of whole-animal biodistribution with enhanced focus on non-traditional NCS cell types and organs, an understanding of the strengths and weaknesses of

nanoparticles regarding physiological interactions, and greater knowledge of the immune and endocytic environment that nanoparticles face, will all assist in the development of next-generation nanoparticles and the field as a whole.

2. Laboratory research: preparation and characterization of liposomes with varying size and composition

2.1. Rationale

Liposomes are attractive candidates for nanodelivery because of their relative ease of preparation, low level of toxicity, and ability to carry a large variety of therapeutics. Further, recent studies have explored the use of liposomes as biological pre-conditioning agents to assist in the effective delivery of other nanoparticle therapies. This brief report is a proof of concept of skills and procedures required for future studies which will explore the kinetics of liposome interactions with cells of the NCS.

2.2. Materials and Methods

Liposomes of two sizes and formulations were produced. First, liposomes were produced with a similar formulation and size to the FDA-approved liposomal cancer therapeutic Doxil.[204] 100nm and 200nm were chosen as two sizes within that range which could be used for comparative purposes in future studies (see Future Directions). DiO liposomes were also made with a similar formulation to FDA-approved liposomal cancer therapeutic Myocet,[204] and 1 mol percent of the hydrophobic, fluorescent green dye DiO was added in a procedure similar to that reported by Mock et al.[205]

The following protocol was used to prepare the 200nm liposomes (200nm Lip):

1. Suspend DSPC, Cholesterol, and DSPE-PEG in chloroform at 10mg/mL.
2. Add 300µL DSPC, 200µL DSPE-PEG, and 100µL Cholesterol to a small round bottom flask in a 4:2 molar ratio with 1 mole percent DiO.
3. Evaporate chloroform from the lipid solution made in round-bottom flask on Roto-Vap.
    a. Turn on all components of Roto-vap and set water bath to 60°C, chiller to 8°C, and the pressure to 70 mbar.
    b. Lower the flask into the water bath making sure that it is submerged far enough to create a wide film, set rotation speed to a setting of 5, and allow chloroform to evaporate (this should take about 5 minutes and a thin film will be formed).
4. Assemble extruder according to manufacturer's instructions.
5. Put assembled extruder, 1X PBS solution, and a small beaker with water in it on a hot plate set to about 120°C. Adjust hot plate temperature to keep the extruder temperature at 70°C.
6. Resuspend the flask in 1mL 1X PBS solution (heated to about 70°C).
7. Put parafilm over top of flask and incubate in small beaker for about one minute.
8. Sonicate flask for about 30 seconds, rotating to hydrate the entire lipid film.
9. Repeat 8-9 until the solution is dispersed completely.
10. Push 1mL PBS through the extruder 5 times to pre-wet filter and check for leaks.
11. Transfer lipid solution from round bottom flask into 1000 µL gas tight syringe for extrusion.
12. Insert the syringe with the lipid solution into one end of the extruder and the other empty syringe into the other end.
13. Wait for about two minutes to let the lipid solution in the syringe reach 70°C.

14. Depress plunger of the filled syringe, passing the lipids through the extruder into the other syringe.
15. Complete 21 passages though the extruder with the solution ending in the syringe that was originally empty. The solution should be clearer.
16. Remove the syringe with the liposome solution from the extruder and transfer the solution into a 1.5 mL tube to be saved for analysis.

The same protocol was used to prepare the 100nm liposomes, except a 100nm polycarbonate filter was used instead of a 200nm polycarbonate filter. For the DiO liposomes, the procedure was also identical except the molar ratio of lipids was 4:2 DSPC to Chol and 1 mol% DiO.

Table 2.1: Materials and equipment used for liposome preparation

Materials/Equipment	Source
DSPC	Avanti Polar Lipids
DSPE-PEG	Avanti Polar Lipids
Cholesterol	Avanti Polar Lipids
DiO	Avanti Polar Lipids
PBS	Sigma-Aldrich
Chloroform	Sigma-Aldrich
Lipid extruder	Avanti Polar Lipids
100 and 200nm polycarbonate filters	Avanti Polar Lipids
Filter supports	Avanti Polar Lipids
RotoVap R-100	Buchi
Zetasizer Nano (DLS)	Malvern Panalytical

3800 Ultrasonic Cleaner	Branson

2.3. Results

5µL of each liposome preparation was mixed with 695µL PBS and analyzed using Dynamic Light Scattering (DLS). The PDI, mean diameter, and zeta potential of the samples measured is reported in Table 1. Each liposome formulation was tested three times. All of these values were in expected ranges. However, it was interesting to note that the sizes did not exactly match the pore sizes of the polycarbonate filters. This is common with liposome preparation by extrusion, and the greater size of the DiO liposomes may have been influenced by greater flexibility due to its formulation, allowing it to deform more when passing through the filter and retain a larger size. To keep the size closer to 100nm, DSPC or a higher molar ratio of cholesterol could be added to the formulation.

Table 2.2: DLS Characterization of nanoparticles with varying size and composition

Sample Name	PDI	Mean diameter (nm)	ZP (mV)
200nm Lip	0.123	164.4	-0.313
200nm Lip	0.107	162.6	-0.396
200nm Lip	0.093	157.7	-0.219
100nm Lip	0.154	125.1	-0.286
100nm Lip	0.120	127.3	-0.169
100nm Lip	0.117	127.4	0.0942
100nm DiO Lip	0.038	141.5	-0.382

100nm DiO Lip	0.070	144.8	-0.210
100nm DiO Lip	0.094	145.6	-0.198

Each liposome formulation was tested three times. 200nm Lip and 100nm Lip refer to the liposomes made from the Doxil-like formulation using 100nm and 200nm polycarbonate filters. 100nm DiO Lip refers to the Myocet-like formulation made using a 100nm polycarbonate filter and DiO.

2.4. Conclusion of laboratory research

Various formulations of liposomes similar to current FDA-approved formulations were prepared and characterized according to standard protocols. These liposomes were made to demonstrate relevant laboratory skills and to explore the formulation of fluorescent liposomes which could be used in future studies (see section 3). The size and zeta potential of the liposomes were successfully quantified via dynamic light scattering.

3. Future directions: Uptake dynamics of liposomes by model NCS cells *in vitro* and proof of concept for use as NCS-blocking pretreatment strategy

The following is an experiment plan developed to test nanoparticle interactions with a model NCS cell. All results and charts are simulated based on expectations of the outcome of each experiment.

3.1. Project Purpose

3.1.1. Background/specific objective

The cells of the NCS, which clear nanoparticles through mechanisms including endocytosis, direct translocation, and NETs, constitute a large barrier to effective nanodelivery. Understanding the kinetics of NCS cellular uptake in order to improve efficacy and mitigate toxicity is important for the development of a wide range of nanoparticle-based therapies. Liposomes have been explored both as drug delivery vehicles for nanomedicine and as preconditioning agents to enhance the delivery of other nanotherapeutics. The objective of this study is to quantify and characterize the uptake dynamics of varying formulations of liposomes in multiple NCS cell models and explore the possibility of saturating the NCS as a pre-treatment for increasing the efficacy of a subsequently administered nanotherapy.

3.1.2. Novelty of the project

- Quantifies the uptake dynamics of multiple liposome formulations for multiple cell types in the same study
- Explores the kinetics of the saturation technique on a cellular level

3.1.3. Scientific questions addressed

- How many liposomes can various NCS cells clear before their clearance function is significantly impaired?
- How do NCS cell clearance dynamics depend on liposome concentration and time?
- How do NCS cell clearance dynamics depend on liposome size?
- Can pre-treatment with liposomes block NCS cells from taking up another nanoparticle?

3.1.4. Key research papers:

Rationales for the first 10 papers are given. These papers were read to inform what characteristics of liposomes will be best for optimizing macrophage uptake. Recommended reading for anyone planning a liposome-based nanoparticle study.

1. Lobatto, M. E. et al. Multimodal Positron Emission Tomography Imaging to Quantify Uptake of 89 Zr-Labeled Liposomes in the Atherosclerotic Vessel Wall. Bioconjug. Chem. acs.bioconjchem.9b00256 (2019). doi:10.1021/acs.bioconjchem.9b00256

-Describes a possible method of labeling liposomes for distribution analysis

2. Niu, G., Cogburn, B. & Hughes, J. Preparation and Characterization of Doxorubicin Liposomes. Cancer Nanotechnol. 624, 211–219 (2010).

-Discusses the protocol and composition of FDA-approved doxorubicin liposomes

3. Takano, S., Aramaki, Y. & Tsuchiya, S. Physicochemical properties of liposomes affecting apoptosis induced by cationic liposomes in macrophages. Pharm. Res. 20, 962–968 (2003).

-Discusses the effect of charged liposomes on cellular processes and uptake. Large positive charges should be avoided.

4. Johnstone, S. A., Masin, D., Mayer, L. & Bally, M. B. Surface-associated serum proteins inhibit the uptake of phosphatidylserine and poly(ethylene glycol) liposomes by mouse macrophages. Biochim. Biophys. Acta - Biomembr. 1513, 25–37 (2001).

-Slightly counterintuitive, but states that the serum proteins that interact with PEG liposomes actually inhibit macrophage uptake. Trials both with FBS and without should be considered.

5. Aoki, H., Fuji, K. & Miyajima, K. Effects of blood on the uptake of charged liposomes by perfused rat liver: Cationic glucosamine-modified liposomes interact with erythrocyte and escape phagocytosis by macrophages. Int. J. Pharm. 149, 15–23 (1997).

-Describes effect of charge on interactions with RBCs. Again, positive charge should be avoided so that liposomes will be taken up by macrophages.

6. Contribution of Kupffer cells to liposome accumulation in the liver. Colloids Surfaces B Biointerfaces 158, 356–362 (2017).

-Described an extremely important cell type for physiological liposome uptake. If primary Kupffer cells cannot be used, RAW264.7 macrophages can be a sufficient proxy.

7. La-Beck, N. M. & Gabizon, A. A. Nanoparticle Interactions with the Immune System: Clinical Implications for Liposome-Based Cancer Chemotherapy. Front. Immunol. 8, 416 (2017).

-A good overview of how liposomes interact with a variety of immune cells, especially macrophages.

8. Petty, H. R. & Francis, J. W. Novel fluorescence method to visualize antibody-dependent hydrogen peroxide-associated 'killing' of liposomes by phagocytes. Biophys. J. 47, 731–734 (1985).

-A good description of an early method for liposome tracking by fluorescence.

9. Levchenko, T. S., Rammohan, R., Lukyanov, A. N., Whiteman, K. R. & Torchilin, V. P. Liposome clearance in mice: The effect of a separate and combined presence of surface charge and polymer coating. Int. J. Pharm. 240, 95–102 (2002).

-Describes how charge and PEG affect the uptake of liposomes in a physiological system. Charged liposomes exhibit greater uptake.

10. Wassef, N. M. & Alving, C. R. Complement-Dependent Phagocytosis of Liposomes by Macrophages. Methods Enzymol. 149, 124–134 (1987).

-Describes the affect of protein corona formation and effect on liposome uptake by macrophages. Macrophages seem to prefer opsonized liposomes, so incubation with FBS may optimize uptake.

11. Allen, T. M. The use of glycolipids and hydrophilic polymers in avoiding rapid uptake of liposomes by the mononuclear phagocyte system. Adv. Drug Deliv. Rev. 13, 285–309 (1994).

12. Chono, S., Tanino, T., Seki, T. & Morimoto, K. Uptake characteristics of liposomes by rat alveolar macrophages: influence of particle size and surface mannose modification. J. Pharm. Pharmacol. 59, 75–80 (2007).

13. Ahsan, F., Rivas, I. P., Khan, M. A. & Torres Suárez, A. I. Targeting to macrophages: Role of physicochemical properties of particulate carriers - Liposomes and microspheres - On the phagocytosis by macrophages. Journal of Controlled Release 79, 29–40 (2002).

14. Wei, M., Zou, Q., Wu, C. & Xu, Y. [In vitro targeting effect of lactoferrin modified PEGylated liposomes for hepatoma cells]. Yao Xue Xue Bao 50, 1272–9 (2015).

15. Samuelsson, E., Shen, H., Blanco, E., Ferrari, M. & Wolfram, J. Contribution of Kupffer cells to liposome accumulation in the liver. Colloids Surfaces B Biointerfaces 158, (2017).

16. Zhang, J. S., Liu, F. & Huang, L. Implications of pharmacokinetic behavior of lipoplex for its inflammatory toxicity. Advanced Drug Delivery Reviews 57, 689–698 (2005).

17. Kelly, C., Jefferies, C. & Cryan, S.-A. Targeted liposomal drug delivery to monocytes and macrophages. J. Drug Deliv. 2011, 727241 (2011).

18. Epstein-Barash, H. et al. Physicochemical parameters affecting liposomal bisphosphonates bioactivity for restenosis therapy: Internalization, cell inhibition, activation of cytokines and complement, and mechanism of cell death. J. Control. Release 146, 182–195 (2010).

19. Petersen, G. H., Alzghari, S. K., Chee, W., Sankari, S. S. & La-Beck, N. M. Meta-analysis of clinical and preclinical studies comparing the anticancer efficacy of liposomal versus conventional non-liposomal doxorubicin. J. Control. Release 232, 255–264 (2016).

20. Wolfram, J. et al. A chloroquine-induced macrophage-preconditioning strategy for improved nanodelivery. Sci. Rep. 7, 13738 (2017).

21. Derksen, J. T. P., Morselt, H. W. M., Kalicharan, D., Hulstaert, C. E. & Scherphof, G. L. Interaction of immunoglobulin-coupled liposomes with rat liver macrophages in vitro. Exp. Cell Res. 168, 105–115 (1987).

22. Kang, K. W. & Song, M. G. Organic Nanomaterials: Liposomes, Albumin, Dendrimer, Polymeric Nanoparticles. in 105–123 (2018). doi:10.1007/978-3-319-67720-0_5

23. Delli Castelli, D. et al. Evidence for in vivo macrophage mediated tumor uptake of paramagnetic/fluorescent liposomes. NMR Biomed. 22, 1084–1092 (2009).

24. Hsu, M. J. & Juliano, R. L. Interactions of liposomes with the reticuloendothelial system. Biochim. Biophys. Acta - Mol. Cell Res. 720, 411–419 (1982).

25. Hu, Q. & Liu, D. Co-existence of serum-dependent and serum-independent mechanisms for liposome clearance and involvement of non-Kupffer cells in liposome uptake by mouse liver. Biochim. Biophys. Acta - Biomembr. 1284, 153–161 (1996).

26. Ahsan, F., Rivas, I. P., Khan, M. A. & Torres Suárez, A. I. Targeting to macrophages: Role of physicochemical properties of particulate carriers - Liposomes and microspheres - On the phagocytosis by macrophages. Journal of Controlled Release 79, 29–40 (2002).

27. Kronberg, B., Dahlman, A., Carlfors, J., Karlsson, J. & Artursson, P. Preparation and evaluation of sterically stabilized liposomes: Colloidal stability, serum stability, macrophage uptake, and toxicity. J. Pharm. Sci. 79, 667–671 (1990).

28. Raz, A., Bucana, C., Fogler, W. E., Poste, G. & Fidler, I. J. Biochemical, Morphological, and Ultrastructural Studies on the Uptake of Liposomes by Murine Macrophages. Cancer Res. 41, 487–494 (1981).

29. Hsu, M. J. & Juliano, R. L. Interactions of liposomes with the reticuloendothelial system. II. Nonspecific and receptor-mediated uptake of liposomes by mouse peritoneal macrophages. BBA - Mol. Cell Res. 720, 411–419 (1982).

30. Allen, T. M., Austin, G. A., Chonn, A., Lin, L. & Lee, K. C. Uptake of liposomes by cultured mouse bone marrow macrophages: influence of liposome composition and size. BBA - Biomembr. 1061, 56–64 (1991).

31. Liu, T., Choi, H., Zhou, R. & Chen, I. W. RES blockade: A strategy for boosting efficiency of nanoparticle drug. Nano Today 10, 11–21 (2015).

3.2. Experimental design

3.2.1. RAW267.4 uptake dynamics of different sizes of liposomes

Rationale

RAW267.4 macrophages will be used as a model of a tissue-resident macrophage. For a list of relevant equipment and materials, refer to Table 2.1. First, fluorescent nanoparticles with sizes of 100 and 200 nm will be prepared with DiO, cholesterol, and DSPG according to the following procedure:

Liposome Preparation

1. Suspend DSPG, Cholesterol, and DiO in chloroform at 10mg/mL.
2. Add DSPG and Cholesterol to a small round bottom flask in a 4:2 molar ratio with 1 mole percent DiO.
3. Evaporate chloroform from the lipid solution made in round-bottom flask on Roto-Vap.
    a. Turn on all components of Roto-vap and set water bath to 60 °C, chiller to 8 °C, and the pressure to 70 mbar.
    b. Lower the flask into the water bath making sure that it is submerged far enough to create a wide film, set rotation speed to a setting of 5, and allow chloroform to evaporate (this should take about 5 minutes and a thin film will be formed).
4. Assemble extruder according to manufacturer's instructions.
5. Put assembled extruder, 1X PBS solution, and a small beaker with water in it on a hot plate set to about 120°C. Adjust hot plate temperature to keep the extruder temperature at 70°C.
6. Resuspend the flask in 1mL 1X PBS solution (heated to about 70°C).

7. Put parafilm over top of flask and incubate in small beaker for about one minute.
8. Sonicate flask for about 30 seconds, rotating to hydrate the entire lipid film.
9. Repeat 8-9 until the solution is dispersed completely.
10. Push 1mL PBS through the extruder 5 times to pre-wet filter and check for leaks.
11. Transfer lipid solution from round bottom flask into 1000 µL gas tight syringe for extrusion.
12. Insert the syringe with the lipid solution into one end of the extruder and the other empty syringe into the other end.
13. Wait for about two minutes to let the lipid solution in the syringe reach 70°C.
14. Depress plunger of the filled syringe, passing the lipids through the extruder into the other syringe.
15. Complete 21 passages though the extruder with the solution ending in the syringe that was originally empty. The solution should be clearer.
16. Remove the syringe with the liposome solution from the extruder and transfer the solution into a 1.5 mL tube to be saved for analysis.

DSPG is used to give the liposomes a negative charge, which will optimize cellular uptake. Cholesterol is used to increase the stiffness and durability of the liposomes. DiO is used as a fluorescent marker to aid in liposome quantification. The concentrations of the stock nanoparticle preparations can be determined by NTA. Alternatively, concentration could be quantified using phospholipid assays. Then, RAW267.4 macrophages will be plated in five 24-well plates and dosed with liposomes according to Figure 3.1. The cells will be washed with PBS and analyzed after 30 minutes, one hour, two hours, four hours, and six hours. If necessary, this procedure will be repeated with different time points for enhanced resolution. If there is high cell

death dose can be decreased, and if uptake approaches total number of liposomes administered, dose can be increased. The cells will be analyzed in a plate reader for fluorescence, and the fluorescence measurements will be correlated to the number concentration of nanoparticles using a standard curve.

Cells + 100nm lip, [1], unwashed	Cells only	100nm lip only	200nm lip only	100nm lip + cells	200nm lip + cells
Cells + 100nm lip, [2], unwashed	Cells only	100nm lip only	200nm lip only	100nm lip + cells	200nm lip + cells
Cells + 100nm lip, [3], unwashed	Cells only	100nm lip only	200nm lip only	100nm lip + cells	200nm lip + cells
Cells + 100nm lip, [4], unwashed	Cells + 200nm lip, [1], unwashed	Cells + 200nm lip, [2], unwashed	Cells + 200nm lip, [3], unwashed	1 Cells + 200nm lip, [4], unwashed	

Figure 3.1: 24-well plate setup for experiment component 2. *[x] corresponds to the four concentrations to be used for the standard curve, which may vary based on the concentration of the stock solution

Expected results

After a certain amount of time, very few additional nanoparticles will be taken up as time goes on. The flattening of the curve at this saturation point is shown in Figure 3.2. This amount

of time needed to reach this point may be different for each size of nanoparticles since size of liposomes can affect uptake efficiency.

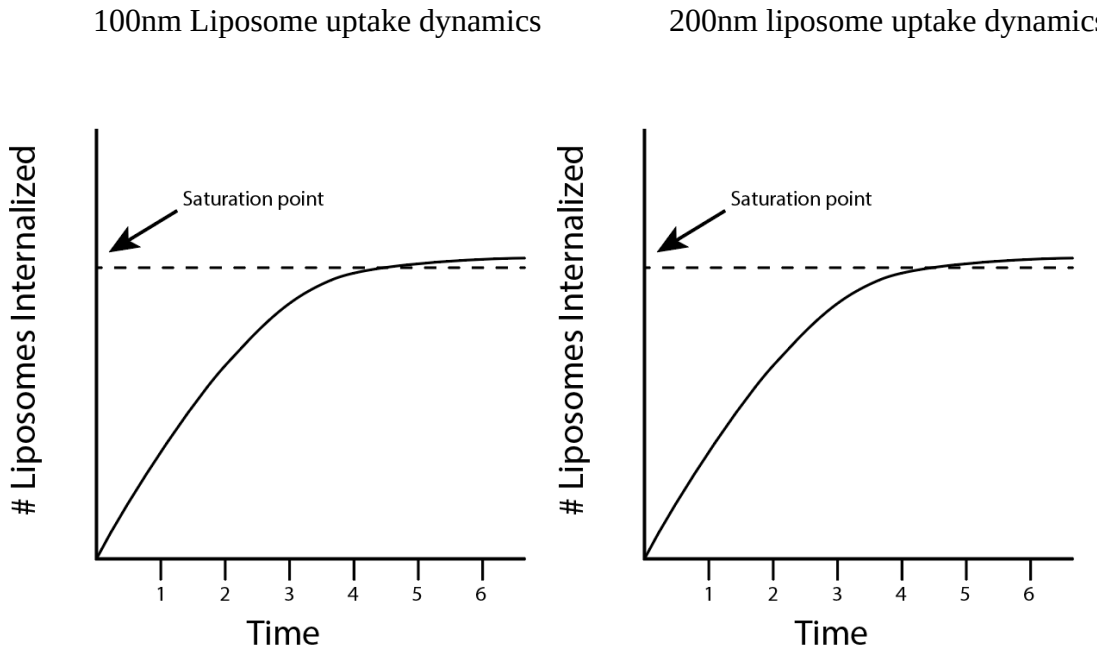

Figure 3.2: Expected results for component 2 – calculation of saturation point

3.2.2 Uptake of AuNPs after saturating dose of liposomes

Rationale

Nanoparticle design characteristics can be modulated to optimize biodistribution for different therapeutic purposes. Therefore, a universal strategy to mitigate NCS interactions regardless of the composition or design of the therapeutic nanoparticle would be highly beneficial. In Figure 3.2, the amount of time necessary for liposomes to saturate RAW267.4 macrophages was reported. The optimum time and nanoparticle size that most quickly saturates

the macrophages will be chosen in this experiment. 50nm AuNPs will be prepared according to standard lab procedure. They will not be PEGylated in order to optimize cell uptake. Cells will be plated in a 12-well plate according to Figure 3.3. They will be pre-dosed with the liposomes from Figure 3.2 which most quickly saturated NCS cells. Then, after the time corresponding to the saturation point has been reached, the cells will be washed and dosed with AuNPs. After 1 hour, 4 hours, and 24 hours, the cells will be washed, harvested, and analyzed via ICP-MS for gold content.

Cells + 50nm AuNP, [1], unwashed	Cells only	Cells + lip + AuNP	Cells + AuNP
Cells + 50nm AuNP, [2], unwashed	Cells only	Cells + lip + AuNP	Cells + AuNP
Cells + 50nm AuNP, [3], unwashed	Cells only	Cells + lip + AuNP	Cells + AuNP

Figure 3.3: 12-well plate setup for experiment component 3

Expected results

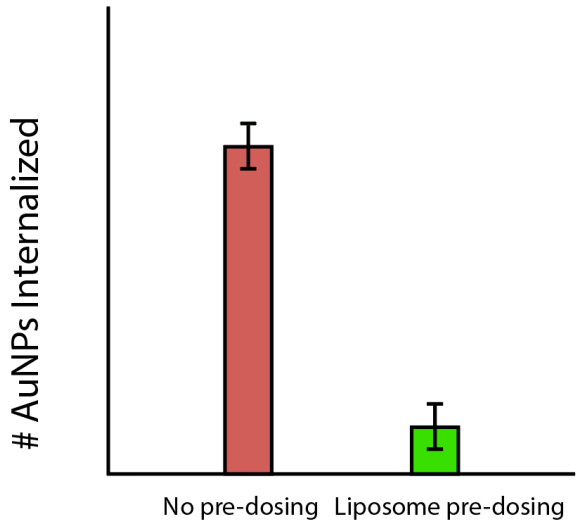

Figure 3.4: Expected results for experiment component 3 – comparison of gold uptake between unmodified and pre-dosed macrophages

3.3. Flow of the components of the project

3.3.1. Basic component flow

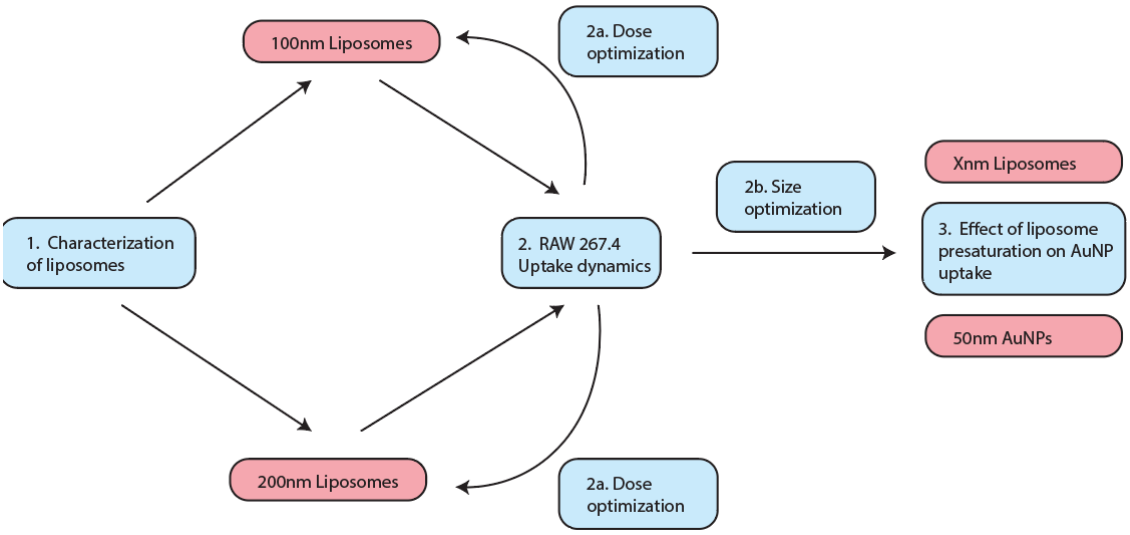

Figure 3.5: Flow of the basic components of the experiment plan

3.3.2. Subcomponent flow

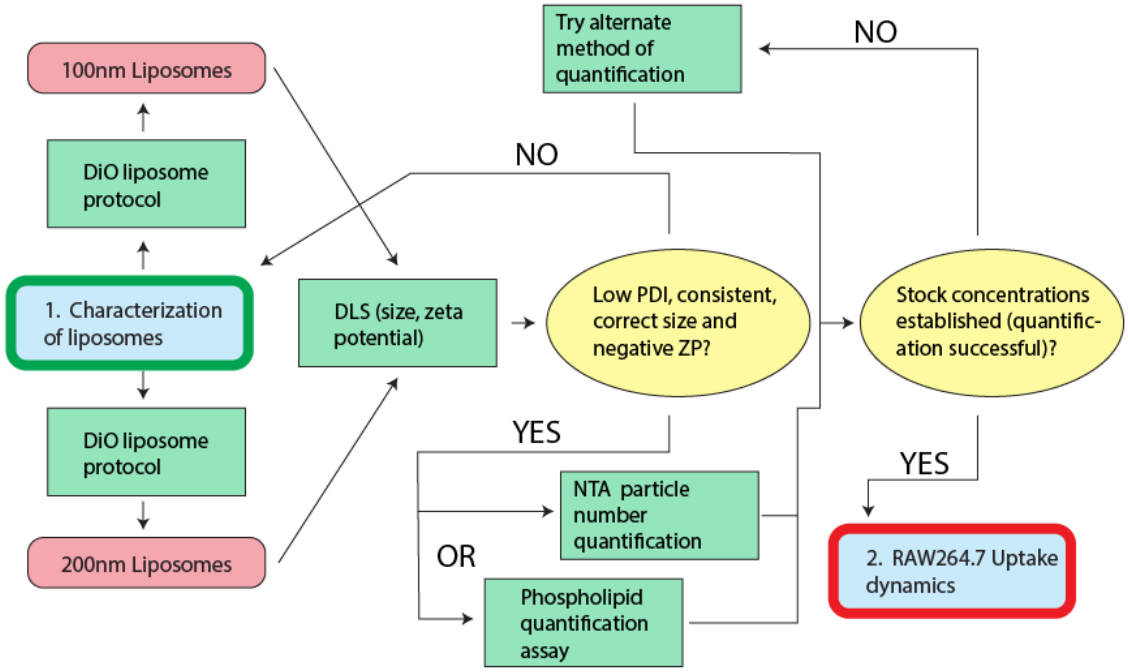

Figure 3.6: Component 1 – preparation and characterization of liposomes

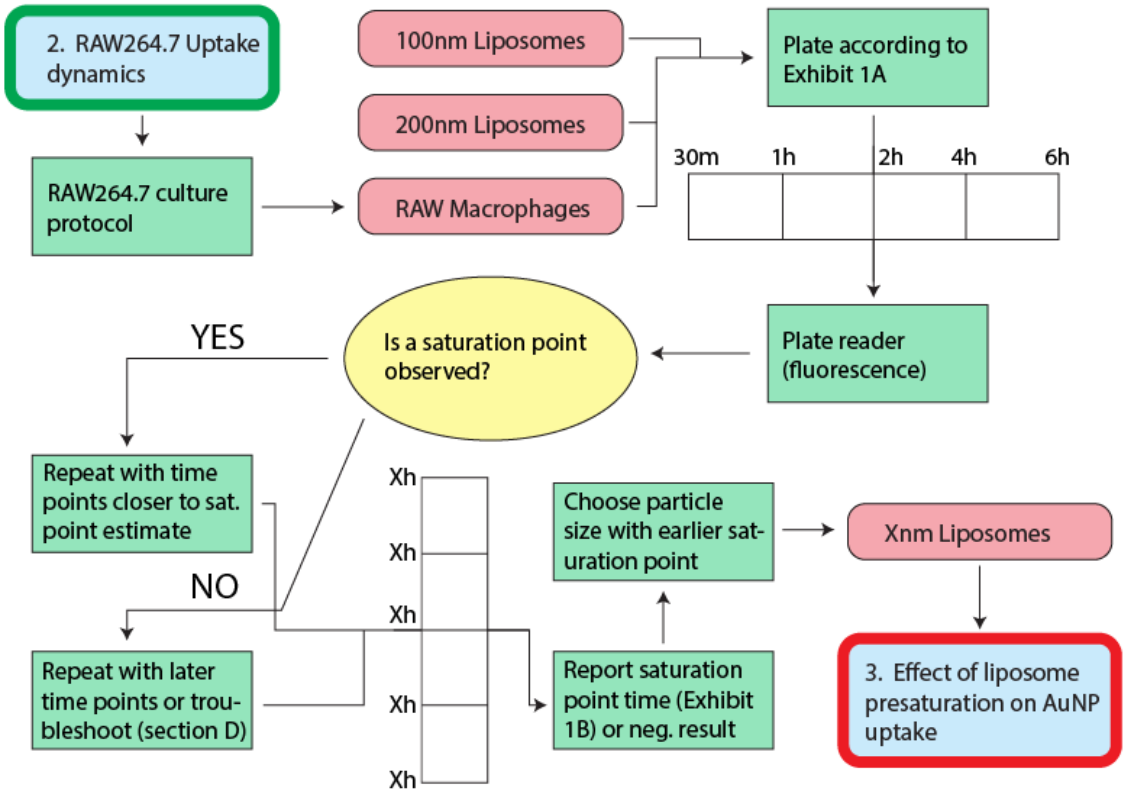

Figure 3.7: Component 2 – RAW264.7 uptake dynamics

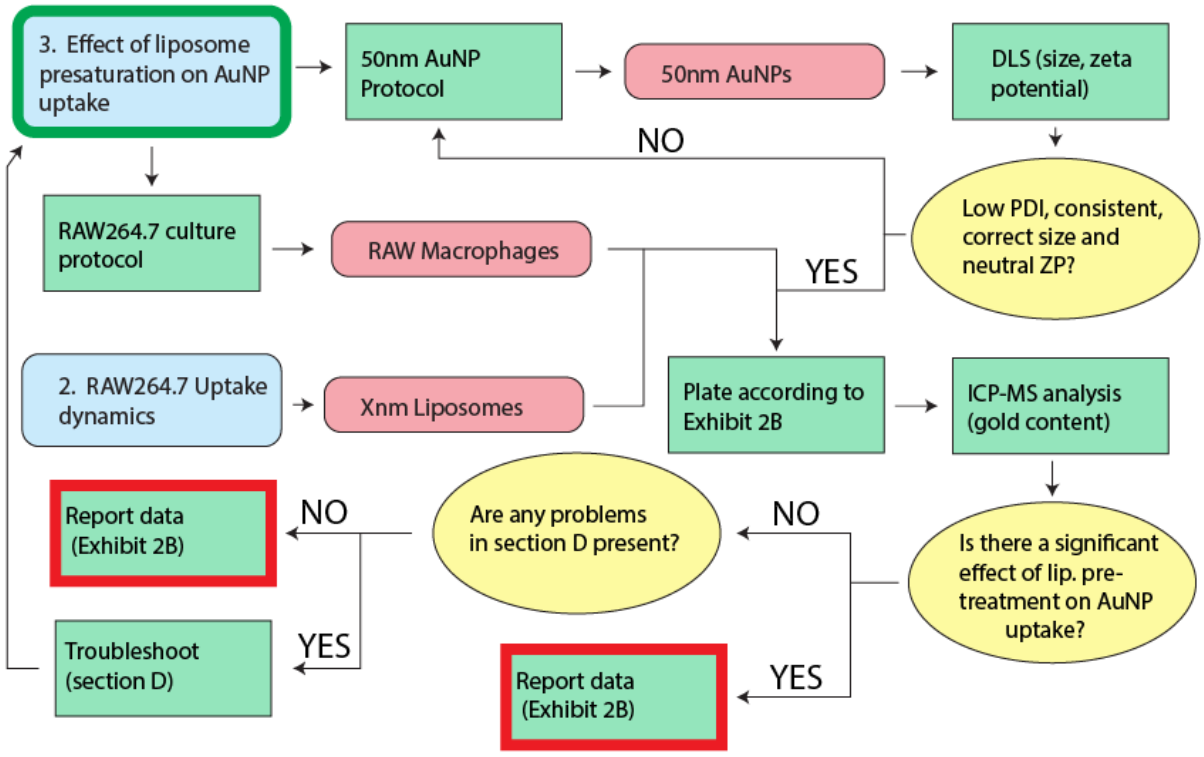

Figure 3.8: Component 3 – effect of liposome presaturation on AuNP uptake

3.4. Conclusion of experiment plan

These experiments were planned for a future study that will quantify gold nanoparticle interactions with a model NCS cells (RAW264.7 macrophages) after they have been saturated with liposomes. The strategy of saturating the NCS with a non-toxic nanoparticle was discussed in section 1.6.1 and identified through literature survey as a promising technique for NCS evasion. By quantifying the interactions of this strategy on a cellular level, the technique can be explored in greater detail and the mechanisms of its efficacy clarified.

4. Conclusion

In this thesis, the need for quantification of nanoparticle interactions with the Nanoparticle Clearance System was established by literature review. Then, a literature survey was used to quantify the differences in organ-level interactions between different nanoparticle formulations. Finally, laboratory experiments were developed and planned to test liposome interactions with a model NCS cell.

In many cases, quantification of nanoparticle interactions with every relevant physiological system is a challenging task: nanoparticles interact differently with NCS organs due to differences in both cell-mediated and cell-independent mechanisms. However, quantitative analysis of interactions with every relevant organ and quantitative tracking of the nanoparticle's residence in different physiological compartments is of utmost importance. Thorough understanding of how nanoparticles move within the body over time is necessary for the continual development of nanoparticle therapeutics with fewer side effects and greater efficacy.

Many contradicting findings regarding how specific nanoparticle characteristics such as material, mechanical properties, size, charge, and surface modifications remain in the literature. These contradictions may result from the complex interplay of synthetic and biological factors, as well as differences in models used for nanoparticle pharmacokinetic studies. Although this makes generalizing biodistribution patterns based on singular characteristics difficult, some patterns emerge and could be useful for the future rational design of nanoparticles. These patterns have been analyzed from a survey of relevant literature, comparing biodistribution data from many different NCS-evading strategies.

One specific NCS-evading strategy, liposomal pre-saturation of the NCS, has been expanded on experimentally. Model liposomes were formulated and characterized using DLS for

size and surface charge. Further, an experimental plan was developed to quantitatively assess the uptake limits of a model NCS cell and how saturating NCS cells may affect their uptake of a model therapeutic nanoparticle (AuNPs). This plan could be used in the future to confirm the potential of such a NCS-saturating strategy.

Overall, the quantitative description of nanoparticle interactions with the NCS and other physiological systems is an attainable and desirable goal to progress the field of nanomedicine. Challenges and knowledge gaps remain, but these represent areas of potential and opportunities for growth. As these gaps are filled in, nanoparticles can be designed with a more guided approach to assure their efficacy and safety. Especially when combined with other fields such as immunology, nanoparticles represent a technological step forward in how medicines are delivered to the body and how a range of disease treatments are approached.

5. Acknowledgements

Special thanks to Grace Le for assisting in the search for some of the articles found in Table 3.

Many thanks to the members of my committee, Dr. Stefan Wilhelm, Dr. Marc Moore, and Dr. Handan Acar, for their support and feedback on this thesis.

6. References

1. Danhier, F. To exploit the tumor microenvironment: Since the EPR effect fails in the clinic, what is the future of nanomedicine? *Journal of Controlled Release* **244**, 108–121 (2016).

2. Zhang, Y.-N., Poon, W., Tavares, A. J., McGilvray, I. D. & Chan, W. C. W. Nanoparticle–liver interactions: Cellular uptake and hepatobiliary elimination. *J. Control. Release* **240**, 332–348 (2016).

3. Wilhelm, S. Analysis of nanoparticle deliery to tumors. *Nat. Rev. Mater.* **1**, 16014 (2016).

4. Wilhelm, S., Tavares, A. J. & Chan, W. C. W. Reply to "Evaluation of nanomedicines: stick to the basics". *Nat. Rev. Mater.* **1**, 16074 (2016).

5. Francia, V. *et al.* Corona Composition Can Affect the Mechanisms Cells Use to Internalize Nanoparticles. *ACS Nano* (2019). doi:10.1021/acsnano.9b03824

6. Yuan, D., He, H., Wu, Y., Fan, J. & Cao, Y. Physiologically Based Pharmacokinetic Modeling of Nanoparticles. *Journal of Pharmaceutical Sciences* **108**, 58–72 (2019).

7. Dai, Q. *et al.* Quantifying the Ligand-Coated Nanoparticle Delivery to Cancer Cells in Solid Tumors. *ACS Nano* **12**, 8423–8435 (2018).

8. Gilleron, J. *et al.* Image-based analysis of lipid nanoparticle-mediated siRNA delivery, intracellular trafficking and endosomal escape. *Nat. Biotechnol.* **31**, 638–646 (2013).

9. Magzoub, M., Jin, S. & Verkman, A. S. Enhanced macromolecule diffusion deep in tumors after enzymatic digestion of extracellular matrix collagen and its associated proteoglycan decorin. *FASEB J.* **22**, 276–284 (2008).

10. Sahay, G., Alakhova, D. Y. & Kabanov, A. V. Endocytosis of nanomedicines. *Journal of Controlled Release* **145**, 182–195 (2010).

11. Lin, J. & Alexander-Katz, A. Cell membranes open 'doors' for cationic nanoparticles/ biomolecules: Insights into uptake kinetics. *ACS Nano* **7**, 10799–10808 (2013).

12. Nejat Pishkenari, H., Barzegar, M. R. & Taghibakhshi, A. Study and Simulation of Nanoparticle Translocation Through Cell Membrane. *Iran. J. Sci. Technol. - Trans. Mech. Eng.* (2019). doi:10.1007/s40997-019-00326-8

13. Bartneck, M., Keul, H. A., Gabriele, Z. K. & Groll, J. Phagocytosis independent extracellular nanoparticle clearance by human immune cells. *Nano Lett.* **10**, 59–64 (2010).

14. Sarker, D. Engineering of Nanoemulsions for Drug Delivery. *Curr. Drug Deliv.* **2**, 297–310 (2005).

15. Kang, K. W. & Song, M. G. Organic Nanomaterials: Liposomes, Albumin, Dendrimer, Polymeric Nanoparticles. in 105–123 (2018). doi:10.1007/978-3-319-67720-0_5

16. Luo, S. *et al.* Carboxyl of Poly(D,L-lactide-co-glycolide) Nanoparticles of Perfluorooctyl Bromide for Ultrasonic Imaging of Tumor. *Contrast Media Mol. Imaging* **2018**, (2018).

17. HALMA, C., DAHA, M. R. & ES, L. A. In vivo clearance by the mononuclear phagocyte system in humans: an overview of methods and their interpretation. *Clin. Exp. Immunol.* **89**, 1–7 (1992).

18. Anderson, C. L. The liver sinusoidal endothelium reappears after being eclipsed by the Kupffer cell: a 20th century biological delusion corrected. (2015). doi:10.1189/jlb.4VMLT0215-054R

19. Wake, K., Kawai, Y. & Smedsrød, B. Re-evaluation of the reticulo-endothelial system. *Ital. J. Anat. Embryol.* **106**, 261–9 (2001).

20. Aschoff, L. Das reticulo-endotheliale System BT - Ergebnisse der Inneren Medizin und Kinderheilkunde: Sechsundzwanzigster Band. in (eds. Kraus, F. et al.) 1–118 (Springer

Berlin Heidelberg, 1924). doi:10.1007/978-3-642-90639-8_1

21. van Furth, R. *et al.* [Mononuclear phagocytic system: new classification of macrophages, monocytes and of their cell line]. *Bull. World Health Organ.* **47**, 651–8 (1972).

22. Yona, S. & Gordon, S. From the Reticuloendothelial to Mononuclear Phagocyte System - The Unaccounted Years. *Front. Immunol.* **6**, 328 (2015).

23. Kawai, Y., Smedsrød, B., Elvevold, K. & Wake, K. Uptake of lithium carmine by sinusoidal endothelial and Kupffer cells of the rat liver: new insights into the classical vital staining and the reticulo-endothelial system. *Cell Tissue Res.* **292**, 395–410 (1998).

24. Smedsrod, B., Pertoft, H., Gustafson, S. & Laurent, T. C. Scavenger functions of the liver endothelial cell. *Biochemical Journal* **266**, 313–327 (1990).

25. Campbell, F. *et al.* Directing Nanoparticle Biodistribution through Evasion and Exploitation of Stab2-Dependent Nanoparticle Uptake. *ACS Nano* **12**, 2138–2150 (2018).

26. Tang, Y. *et al.* Overcoming the Reticuloendothelial System Barrier to Drug Delivery with a “Don’t-Eat-Us” Strategy. *ACS Nano* (2019). doi:10.1021/ACSNANO.9B05679

27. Chong, S. Z., Evrard, M., Goh, C. C. & Ng, L. G. Illuminating the covert mission of mononuclear phagocytes in their regional niches. *Curr. Opin. Immunol.* **50**, 94–101 (2018).

28. Guilliams, M. *et al.* Dendritic cells, monocytes and macrophages: a unified nomenclature based on ontogeny. *Nat. Rev. Immunol.* **14**, 571–578 (2014).

29. Gaharwar, U. S., Meena, R. & Rajamani, P. Iron oxide nanoparticles induced cytotoxicity, oxidative stress and DNA damage in lymphocytes. *J. Appl. Toxicol.* **37**, 1232–1244

(2017).

30. Canaday, D. H. *et al.* Capable of Professional Phagocytosis T Cells: A Lymphoid Lineage Cell δ γ Human. *J Immunol* **183**, 5622–5629 (2009).

31. Ahsan, S. M., Rao, C. M. & Ahmad, M. F. Nanoparticle-protein interaction: The significance and role of protein corona. in *Advances in Experimental Medicine and Biology* **1048**, 175–198 (Springer New York LLC, 2018).

32. Hamad, I. *et al.* Distinct Polymer Architecture Mediates Switching of Complement Activation Pathways at the Nanosphere−Serum Interface: Implications for Stealth Nanoparticle Engineering. *ACS Nano* **4**, 6629–6638 (2010).

33. Tavano, R. *et al.* C1q-Mediated Complement Activation and C3 Opsonization Trigger Recognition of Stealth Poly(2-methyl-2-oxazoline)-Coated Silica Nanoparticles by Human Phagocytes. *ACS Nano* **12**, 5834–5847 (2018).

34. Chen, F. *et al.* Complement proteins bind to nanoparticle protein corona and undergo dynamic exchange in vivo. *Nat. Nanotechnol.* **12**, 387–393 (2017).

35. Donahue, N. D., Acar, H. & Wilhelm, S. Concepts of nanoparticle cellular uptake, intracellular trafficking, and kinetics in nanomedicine. *Adv. Drug Deliv. Rev.* (2019). doi:10.1016/J.ADDR.2019.04.008

36. Mahmoudi, M., Bertrand, N., Zope, H. & Farokhzad, O. C. Emerging understanding of the protein corona at the nano-bio interfaces. *Nano Today* **11**, 817–832 (2016).

37. Blanco, E., Shen, H. & Ferrari, M. Principles of nanoparticle design for overcoming biological barriers to drug delivery. *Nat. Biotechnol.* **33**, 941–951 (2015).

38. Dobrovolskaia, M. A., Aggarwal, P., Hall, J. B. & McNeil, S. E. Preclinical Studies To Understand Nanoparticle Interaction with the Immune System and Its Potential Effects on Nanoparticle Biodistribution. *Mol. Pharm.* **5**, 487–495 (2008).

39. Betker, J. L. *et al.* Nanoparticle uptake by circulating leukocytes: A major barrier to tumor delivery. *J. Control. Release* **286**, 85–93 (2018).

40. Lobatto, M. E. *et al.* Multimodal Positron Emission Tomography Imaging to Quantify Uptake of ^{89} Zr-Labeled Liposomes in the Atherosclerotic Vessel Wall. *Bioconjug. Chem.* acs.bioconjchem.9b00256 (2019). doi:10.1021/acs.bioconjchem.9b00256

41. Zhao, Y. *et al.* Interaction of Mesoporous Silica Nanoparticles with Human Red Blood Cell Membranes: Size and Surface Effects. *ACS Nano* **5**, 1366–1375 (2011).

42. Wang, T., Bai, J., Jiang, X. & Nienhaus, G. U. Cellular Uptake of Nanoparticles by Membrane Penetration: A Study Combining Confocal Microscopy with FTIR Spectroelectrochemistry. *ACS Nano* **6**, 1251–1259 (2012).

43. Anselmo, A. C. *et al.* Delivering Nanoparticles to Lungs while Avoiding Liver and Spleen through Adsorption on Red Blood Cells. *ACS Nano* **7**, 11129–11137 (2013).

44. Yang, Y.-W. & Luo, W.-H. Cellular biodistribution of polymeric nanoparticles in the immune system. *J. Control. Release* **227**, 82–93 (2016).

45. Tsoi, K. M. *et al.* Mechanism of hard-nanomaterial clearance by the liver. *Nat. Mater.* **15**, 1212–1221 (2016).

46. Boxenbaum, H. *lnterspecies Variation in Liver Weight, Hepatic Blood Flow, and Antipyrine Intrinsic Clearance: Extrapolation of Data to Benzodiazepines and Phenytoin*.

Journal of Pharmacokinetics and Biopharmaceutics **8**, (1980).

47. Woodhouse, K. W. & Wynne, H. A. Age-Related Changes in Liver Size and Hepatic Blood Flow. *Clin. Pharmacokinet.* **15**, 287–294 (1988).

48. Eipel, C., Abshagen, K. & Vollmar, B. Regulation of hepatic blood flow: the hepatic arterial buffer response revisited. *World J. Gastroenterol.* **16**, 6046–57 (2010).

49. Chadburn, A. The spleen: Anatomy and anatomical function. *Semin. Hematol.* **37**, 13–21 (2000).

50. Mebius, R. E. & Kraal, G. Structure and function of the spleen. *Nat. Rev. Immunol.* **5**, 606–616 (2005).

51. Cesta, M. F. Normal Structure, Function, and Histology of the Spleen. *Toxicol. Pathol.* **34**, 455–465 (2006).

52. Arnon, T. I., Horton, R. M., Grigorova, I. L. & Cyster, J. G. Visualization of splenic marginal zone B-cell shuttling and follicular B-cell egress. *Nature* **493**, 684–688 (2013).

53. Demoy, M. *et al.* Spleen Capture of Nanoparticles: Influence of Animal Species and Surface Characteristics. *Pharm. Res.* **16**, 37–41 (1999).

54. Moghimi, S. M., Porter, C. J. H., Muir, I. S., Illum, L. & Davis, S. S. Non-phagocytic uptake of intravenously injected microspheres in rat spleen: Influence of particle size and hydrophilic coating. *Biochem. Biophys. Res. Commun.* **177**, 861–866 (1991).

55. Zhang, L. *et al.* Softer Zwitterionic Nanogels for Longer Circulation and Lower Splenic Accumulation. *ACS Nano* **6**, 6681–6686 (2012).

56. Chapter 4. Blood Flow to the Lung | Pulmonary Physiology, 8e | AccessMedicine |

McGraw-Hill Medical. Available at: https://accessmedicine.mhmedical.com/content.aspx?bookid=575&sectionid=42512982. (Accessed: 28th August 2019)

57. Brain, J. D. Mechanisms, measurement, and significance of lung macrophage function. *Environ. Health Perspect.* **97**, 5–10 (1992).

58. Warner, A. E. & Brain, J. D. The cell biology and pathogenic role of pulmonary intravascular macrophages. *Am. J. Physiol.* **258**, L1-12 (1990).

59. CRAPO, J. D., HARMSEN, A. G., SHERMAN, M. P. & MUSSON, R. A. Pulmonary Immunobiology and Inflammation in Pulmonary Diseases. *Am. J. Respir. Crit. Care Med.* **162**, 1983–1986 (2000).

60. Ruge, C. A. *et al.* Uptake of nanoparticles by alveolar macrophages is triggered by surfactant protein A. *Nanomedicine Nanotechnology, Biol. Med.* **7**, 690–693 (2011).

61. Chono, S., Tanino, T., Seki, T. & Morimoto, K. Uptake characteristics of liposomes by rat alveolar macrophages: influence of particle size and surface mannose modification. *J. Pharm. Pharmacol.* **59**, 75–80 (2007).

62. Travlos, G. S. Normal Structure, Function, and Histology of the Bone Marrow. *Toxicol. Pathol.* **34**, 548–565 (2006).

63. Abboud, C. . & Lichtman, M. . Structure of the marrow and the hematopoietic microenvironment. in *Williams' Hematology* 29–58 (McGraw-Hill, 2001).

64. Allen, T. D. & Dexter, T. M. The essential cells of the hemopoietic microenvironment. *Exp. Hematol.* **12**, 517–21 (1984).

65. Geoffroy, J. S. & Becker, R. P. Endocytosis by endothelial phagocytes: uptake of bovine serum albumin-gold conjugates in bone marrow. *J. Ultrasructure Res.* **89**, 223–239 (1984).

66. Gottlieb, Y. *et al.* Physiologically aged red blood cells undergo erythrophagocytosis in vivo but not in vitro. *Haematologica* **97**, 994–1002 (2012).

67. Porter, C. J. H., Moghimi, S. M., Illum, L. & Davis, S. S. The polyoxyethylene/polyoxypropylene block co-polymer Poloxamer-407 selectively redirects intravenously injected microspheres to sinusoidal endothelial cells of rabbit bone marrow. *FEBS Lett.* **305**, 62–66 (1992).

68. Yang, Y. W. & Luo, W. H. Recruitment of bone marrow CD11b+ Gr-1+ cells by polymeric nanoparticles for antigen cross-presentation. *Sci. Rep.* **7**, 1–13 (2017).

69. Walters, K. A., Roberts, M. S. & Roberts, M. S. The Structure and Function of Skin. 18–58 (2002). doi:10.4324/9780203910740-7

70. Kumar, R. *et al.* In vivo biodistribution and clearance studies using multimodal organically modified silica nanoparticles. in *ACS Nano* **4**, 699–708 (2010).

71. Yang, R. S. H. *et al.* Persistent tissue kinetics and redistribution of nanoparticles, quantum Dot 705, in Mice: ICP-MS quantitative assessment. *Environ. Health Perspect.* **115**, 1339–1343 (2007).

72. Akiyama, Y., Mori, T., Katayama, Y. & Niidome, T. The effects of PEG grafting level and injection dose on gold nanorod biodistribution in the tumor-bearing mice. *J. Control. Release* **139**, 81–84 (2009).

73. Sykes, E. A., Dai, Q., Tsoi, K. M., Hwang, D. M. & Chan, W. C. W. Nanoparticle exposure in animals can be visualized in the skin and analysed via skin biopsy. *Nat. Commun.* **5**, (2014).

74. Gray, E. E. & Cyster, J. G. Lymph Node Macrophages. *J. Innate Immun.* **4**, 424–436 (2012).

75. Zhang, Y. N. *et al.* Nanoparticle Size Influences Antigen Retention and Presentation in Lymph Node Follicles for Humoral Immunity. *Nano Lett.* **19**, 7226–7235 (2019).

76. Réty, F. *et al.* MR lymphography using iron oxide nanoparticles in rats: Pharmacokinetics in the lymphatic system after intravenous injection. *J. Magn. Reson. Imaging* **12**, 734–739 (2000).

77. Ernsting, M. J., Murakami, M., Roy, A. & Li, S.-D. Factors controlling the pharmacokinetics, biodistribution and intratumoral penetration of nanoparticles. *J. Control. Release* **172**, 782–794 (2013).

78. Wyss, P. P. *et al.* Renal clearance of polymeric nanoparticles by mimicry of glycan surface of viruses. *Biomaterials* **230**, 119643 (2020).

79. Du, B., Yu, M. & Zheng, J. Transport and interactions of nanoparticles in the kidneys. *Nature Reviews Materials* **3**, 358–374 (2018).

80. Weissleder, R. & Pittet, M. J. The expanding landscape of inflammatory cells affecting cancer therapy. *Nat. Biomed. Eng.* (2020). doi:10.1038/s41551-020-0524-y

81. Delli Castelli, D. *et al.* Evidence for in vivo macrophage mediated tumor uptake of paramagnetic/fluorescent liposomes. *NMR Biomed.* **22**, 1084–1092 (2009).

82. Fidler, I. J. Targeting of immunomodulators to mononuclear phagocytes for therapy of cancer. *Advanced Drug Delivery Reviews* **2**, 69–106 (1988).

83. Ahsan, F., Rivas, I. P., Khan, M. A. & Torres Suárez, A. I. Targeting to macrophages: Role of physicochemical properties of particulate carriers - Liposomes and microspheres - On the phagocytosis by macrophages. *Journal of Controlled Release* **79**, 29–40 (2002).

84. Zhao, Z., Ukidve, A., Krishnan, V. & Mitragotri, S. Effect of physicochemical and surface properties on in vivo fate of drug nanocarriers. *Adv. Drug Deliv. Rev.* **143**, 3–21 (2019).

85. Francia, V., Montizaan, D. & Salvati, A. Interactions at the cell membrane and pathways of internalization of nano-sized materials for nanomedicine. *Beilstein J. Nanotechnol.* **11**, 338–353 (2020).

86. Takano, S., Aramaki, Y. & Tsuchiya, S. Physicochemical properties of liposomes affecting apoptosis induced by cationic liposomes in macrophages. *Pharm. Res.* **20**, 962–968 (2003).

87. Guo, D., Xie, G. & Luo, J. Mechanical properties of nanoparticles: Basics and applications. *Journal of Physics D: Applied Physics* **47**, (2014).

88. Hui, Y. *et al.* Role of Nanoparticle Mechanical Properties in Cancer Drug Delivery. *ACS Nano* **13**, 7410–7424 (2019).

89. Anselmo, A. C. *et al.* Elasticity of nanoparticles influences their blood circulation, phagocytosis, endocytosis, and targeting. *ACS Nano* **9**, 3169–3177 (2015).

90. Guo, P. *et al.* Nanoparticle elasticity directs tumor uptake. *Nat. Commun.* **9**, (2018).

91. Sun, J. *et al.* Tunable rigidity of (polymeric core)-(lipid shell) nanoparticles for regulated

cellular uptake. *Adv. Mater.* **27**, 1402–7 (2015).

92. Shen, Z., Ye, H., Yi, X. & Li, Y. Membrane Wrapping Efficiency of Elastic Nanoparticles during Endocytosis: Size and Shape Matter. *ACS Nano* **13**, 215–228 (2019).

93. Hui, Y. *et al.* Understanding the Effects of Nanocapsular Mechanical Property on Passive and Active Tumor Targeting. *ACS Nano* **12**, 2846–2857 (2018).

94. Oberdörster, G. *et al.* Principles for characterizing the potential human health effects from exposure to nanomaterials: elements of a screening strategy. *Part. Fibre Toxicol.* **2**, 8 (2005).

95. Gliga, A. R., Skoglund, S., Odnevall Wallinder, I., Fadeel, B. & Karlsson, H. L. Size-dependent cytotoxicity of silver nanoparticles in human lung cells: the role of cellular uptake, agglomeration and Ag release. *Part. Fibre Toxicol.* **11**, 11 (2014).

96. Albanese, A., Tang, P. S. & Chan, W. C. W. The Effect of Nanoparticle Size, Shape, and Surface Chemistry on Biological Systems. *Annu. Rev. Biomed. Eng.* **14**, 1–16 (2012).

97. Lim, J., Yeap, S. P., Che, H. X. & Low, S. C. Characterization of magnetic nanoparticle by dynamic light scattering. *Nanoscale Res. Lett.* **8**, 1–14 (2013).

98. Wei, Y., Quan, L., Zhou, C. & Zhan, Q. Factors relating to the biodistribution & clearance of nanoparticles & their effects on in vivo application. *Nanomedicine* **13**, 1495–1512 (2018).

99. Soo Choi, H. *et al.* Renal clearance of quantum dots. *Nat. Biotechnol.* **25**, 1165–1170 (2007).

100. De Jong, W. H. *et al.* Particle size-dependent organ distribution of gold nanoparticles after

intravenous administration. *Biomaterials* **29**, 1912–1919 (2008).

101. Li, X. *et al.* The systematic evaluation of size-dependent toxicity and multi-time biodistribution of gold nanoparticles. *Colloids Surfaces B Biointerfaces* **167**, 260–266 (2018).

102. Mandl, H. K. *et al.* Optimizing Biodegradable Nanoparticle Size for Tissue-Specific Delivery. *J. Control. Release* (2019). doi:10.1016/j.jconrel.2019.09.020

103. He, C., Hu, Y., Yin, L., Tang, C. & Yin, C. Effects of particle size and surface charge on cellular uptake and biodistribution of polymeric nanoparticles. *Biomaterials* **31**, 3657–3666 (2010).

104. García-Álvarez, R., Hadjidemetriou, M., Sánchez-Iglesias, A., Liz-Marzán, L. M. & Kostarelos, K. In vivo formation of protein corona on gold nanoparticles. the effect of their size and shape. *Nanoscale* **10**, 1256–1264 (2018).

105. Champion, J. A. & Mitragotri, S. Shape Induced Inhibition of Phagocytosis of Polymer Particles. *Pharm. Res.* **26**, 244–249 (2009).

106. Geng, Y. *et al.* Shape effects of filaments versus spherical particles in flow and drug delivery. (2007). doi:10.1038/nnano.2007.70

107. Huang, X. *et al.* The shape effect of mesoporous silica nanoparticles on biodistribution, clearance, and biocompatibility in vivo. in *ACS Nano* **5**, 5390–5399 (2011).

108. Fornaguera, C. & Solans, C. Characterization of Polymeric Nanoparticle Dispersions for Biomedical Applications: Size, Surface Charge and Stability. *Pharm. Nanotechnol.* **6**, 147–164 (2018).

109. Li, S.-D. & Huang, L. Pharmacokinetics and biodistribution of nanoparticles. *Mol. Pharm.* **5**, 496–504 (2008).

110. Levchenko, T. S., Rammohan, R., Lukyanov, A. N., Whiteman, K. R. & Torchilin, V. P. Liposome clearance in mice: The effect of a separate and combined presence of surface charge and polymer coating. *Int. J. Pharm.* **240**, 95–102 (2002).

111. Zhang, J. S., Liu, F. & Huang, L. Implications of pharmacokinetic behavior of lipoplex for its inflammatory toxicity. *Advanced Drug Delivery Reviews* **57**, 689–698 (2005).

112. Elci, S. G. *et al.* Surface Charge Controls the Suborgan Biodistributions of Gold Nanoparticles. *ACS Nano* **10**, 5536–5542 (2016).

113. Kou, L., Sun, J., Zhai, Y. & He, Z. The endocytosis and intracellular fate of nanomedicines: Implication for rational design. *Asian J. Pharm. Sci.* **8**, 1–10 (2013).

114. Zhao, Z., Ukidve, A., Krishnan, V. & Mitragotri, S. Effect of physicochemical and surface properties on in vivo fate of drug nanocarriers. *Adv. Drug Deliv. Rev.* (2019). doi:10.1016/j.addr.2019.01.002

115. Storm, G., Belliot, S. O., Daemen, T. & Lasic, D. D. Surface modification of nanoparticles to oppose uptake by the mononuclear phagocyte system. *Advanced Drug Delivery Reviews* **17**, 31–48 (1995).

116. Pelaz, B. *et al.* Surface Functionalization of Nanoparticles with Polyethylene Glycol: Effects on Protein Adsorption and Cellular Uptake. *ACS Nano* **9**, 6996–7008 (2015).

117. Shah, N. B. *et al.* Blood–Nanoparticle Interactions and *in Vivo* Biodistribution: Impact of Surface PEG and Ligand Properties. *Mol. Pharm.* **9**, 2146–2155 (2012).

118. Dai, Q., Walkey, C. & Chan, W. C. W. Polyethylene glycol backfilling mitigates the negative impact of the protein corona on nanoparticle cell targeting. *Angew. Chemie - Int. Ed.* **53**, 5093–5096 (2014).

119. Kah, J. C. Y. *et al.* Critical parameters in the pegylation of gold nanoshells for biomedical applications: An in vitro macrophage study. *J. Drug Target.* **17**, 181–193 (2009).

120. Bazile, D. *et al.* Stealth Me. PEG-PLA Nanoparticles Avoid Uptake by the Mononuclear Phagocytes System. *J. Pharm. Sci.* **84**, 493–498 (1995).

121. Allen, T. M. The use of glycolipids and hydrophilic polymers in avoiding rapid uptake of liposomes by the mononuclear phagocyte system. *Adv. Drug Deliv. Rev.* **13**, 285–309 (1994).

122. Mishra, P., Nayak, B. & Dey, R. . PEGylation in anti-cancer therapy: An overview. *Asian J. Pharm. Sci.* **11**, 337–348 (2016).

123. Grenier, P. Anti-polyethylene glycol antibodies alter the protein corona deposited on nanoparticles and the physiological pathways regulating their fate in vivo. *J. Control. Release* **287**, 121–131 (2018).

124. Li, Y., Kröger, M. & Liu, W. K. Endocytosis of PEGylated nanoparticles accompanied by structural and free energy changes of the grafted polyethylene glycol. *Biomaterials* **35**, 8467–8478 (2014).

125. Larson, T. A., Joshi, P. P. & Sokolov, K. Preventing protein adsorption and macrophage uptake of gold nanoparticles via a hydrophobic shield. *ACS Nano* **6**, 9182–9190 (2012).

126. Saha, K. *et al.* Regulation of Macrophage Recognition through the Interplay of

Nanoparticle Surface Functionality and Protein Corona. *ACS Nano* **10**, 4421–4430 (2016).

127. Debayle, M. *et al.* Zwitterionic polymer ligands: an ideal surface coating to totally suppress protein-nanoparticle corona formation? *Biomaterials* **219**, 119357 (2019).

128. Tatumi, R. & Fujihara, H. Remarkably stable gold nanoparticles functionalized with a zwitterionic liquid based on imidazolium sulfonate in a high concentration of aqueous electrolyte and ionic liquid. *Chem. Commun.* 83–85 (2005). doi:10.1039/b413385d

129. Dembele, F. *et al.* Zwitterionic Silane Copolymer for Ultra-Stable and Bright Biomolecular Probes Based on Fluorescent Quantum Dot Nanoclusters. *ACS Appl. Mater. Interfaces* **9**, 18161–18169 (2017).

130. Knowles, B. R., Wagner, P., Maclaughlin, S., Higgins, M. J. & Molino, P. J. Silica Nanoparticles Functionalized with Zwitterionic Sulfobetaine Siloxane for Application as a Versatile Antifouling Coating System. *ACS Appl. Mater. Interfaces* **9**, 18584–18594 (2017).

131. García, K. P. *et al.* Zwitterionic-Coated "Stealth" Nanoparticles for Biomedical Applications: Recent Advances in Countering Biomolecular Corona Formation and Uptake by the Mononuclear Phagocyte System. *Small* **10**, 2516–2529 (2014).

132. Estephan, Z. G., Jaber, J. A. & Schlenoff, J. B. Zwitterion-stabilized silica nanoparticles: Toward nonstick nano. *Langmuir* **26**, 16884–16889 (2010).

133. Arvizo, R. R. *et al.* Modulating Pharmacokinetics, Tumor Uptake and Biodistribution by Engineered Nanoparticles. *PLoS One* **6**, e24374 (2011).

134. Pitek, A. S., Jameson, S. A., Veliz, F. A., Shukla, S. & Steinmetz, N. F. Serum albumin

'camouflage' of plant virus based nanoparticles prevents their antibody recognition and enhances pharmacokinetics. *Biomaterials* **89**, 89–97 (2016).

135. Mann, A. P. *et al.* E-selectin-targeted porous silicon particle for nanoparticle delivery to the bone marrow. *Adv. Mater.* **23**, (2011).

136. Qie, Y. *et al.* Surface modification of nanoparticles enables selective evasion of phagocytic clearance by distinct macrophage phenotypes. *Sci. Rep.* **6**, 26269 (2016).

137. Gulati, N. M., Stewart, P. L. & Steinmetz, N. F. Bioinspired Shielding Strategies for Nanoparticle Drug Delivery Applications. *Mol. Pharm.* **15**, 2900–2909 (2018).

138. Li, H. *et al.* Size Dependency of Circulation and Biodistribution of Biomimetic Nanoparticles: Red Blood Cell Membrane-Coated Nanoparticles. *Cells* **8**, 881 (2019).

139. Yi, X., Shi, X. & Gao, H. Cellular uptake of elastic nanoparticles. *Phys. Rev. Lett.* **107**, 098101 (2011).

140. Lorenz, S. *et al.* The Softer and More Hydrophobic the Better: Influence of the Side Chain of Polymethacrylate Nanoparticles for Cellular Uptake. *Macromol. Biosci.* **10**, 1034–1042 (2010).

141. Venkataraman, S. *et al.* The effects of polymeric nanostructure shape on drug delivery. *Advanced Drug Delivery Reviews* **63**, 1228–1246 (2011).

142. Kelf, T. A. *et al.* Non-specific cellular uptake of surface-functionalized quantum dots. *Nanotechnology* **21**, (2010).

143. Time to deliver. *Nature Biotechnology* **32**, 961 (2014).

144. Akinc, A. & Battaglia, G. Exploiting endocytosis for nanomedicines. *Cold Spring Harbor*

Perspectives in Biology **5**, a016980 (2013).

145. Lerch, S., Dass, M., Musyanovych, A., Landfester, K. & Mailänder, V. Polymeric nanoparticles of different sizes overcome the cell membrane barrier. *Eur. J. Pharm. Biopharm.* **84**, 265–274 (2013).

146. Rejman, J., Oberle, V., Zuhorn, I. S. & Hoekstra, D. Size-dependent internalization of particles via the pathways of clathrin-and caveolae-mediated endocytosis. *Biochem. J.* **377**, 159–169 (2004).

147. Duan, X. & Li, Y. Physicochemical Characteristics of Nanoparticles Affect Circulation, Biodistribution, Cellular Internalization, and Trafficking. *Small* **9**, 1521–1532 (2013).

148. Gratton, S. E. A. *et al.* The effect of particle design on cellular internalization pathways. *Proc. Natl. Acad. Sci. U. S. A.* **105**, 11613–11618 (2008).

149. Kirchhausen, T., Owen, D. & Harrison, S. C. Molecular structure, function, and dynamics of clathrin-mediated membrane traffic. *Cold Spring Harb. Perspect. Biol.* **6**, a016725 (2014).

150. Saffarian, S., Cocucci, E. & Kirchhausen, T. Distinct Dynamics of Endocytic Clathrin-Coated Pits and Coated Plaques. *PLoS Biol.* **7**, e1000191 (2009).

151. Lai, S. K. *et al.* Privileged delivery of polymer nanoparticles to the perinuclear region of live cells via a non-clathrin, non-degradative pathway. *Biomaterials* **28**, 2876–2884 (2007).

152. Agarwal, R. *et al.* Mammalian cells preferentially internalize hydrogel nanodiscs over nanorods and use shape-specific uptake mechanisms. *Proc. Natl. Acad. Sci. U. S. A.* **110**,

17247–17252 (2013).

153. Fotin, A. *et al.* Molecular model for a complete clathrin lattice from electron cryomicroscopy. *Nature* **432**, 573–579 (2004).

154. Wassef, N. M. & Alving, C. R. Complement-Dependent Phagocytosis of Liposomes by Macrophages. *Methods Enzymol.* **149**, 124–134 (1987).

155. Derksen, J. T. P., Morselt, H. W. M., Kalicharan, D., Hulstaert, C. E. & Scherphof, G. L. Interaction of immunoglobulin-coupled liposomes with rat liver macrophages in vitro. *Exp. Cell Res.* **168**, 105–115 (1987).

156. Hsu, M. J. & Juliano, R. L. Interactions of liposomes with the reticuloendothelial system. *Biochim. Biophys. Acta - Mol. Cell Res.* **720**, 411–419 (1982).

157. Petty, H. R. & Francis, J. W. Novel fluorescence method to visualize antibody-dependent hydrogen peroxide-associated 'killing' of liposomes by phagocytes. *Biophys. J.* **47**, 731–734 (1985).

158. Hu, Q. & Liu, D. Co-existence of serum-dependent and serum-independent mechanisms for liposome clearance and involvement of non-Kupffer cells in liposome uptake by mouse liver. *Biochim. Biophys. Acta - Biomembr.* **1284**, 153–161 (1996).

159. Aoki, H., Fuji, K. & Miyajima, K. Effects of blood on the uptake of charged liposomes by perfused rat liver: Cationic glucosamine-modified liposomes interact with erythrocyte and escape phagocytosis by macrophages. *Int. J. Pharm.* **149**, 15–23 (1997).

160. Johnstone, S. A., Masin, D., Mayer, L. & Bally, M. B. Surface-associated serum proteins inhibit the uptake of phosphatidylserine and poly(ethylene glycol) liposomes by mouse

macrophages. *Biochim. Biophys. Acta - Biomembr.* **1513**, 25–37 (2001).

161. Kunjachan, S. *et al.* Passive versus active tumor targeting using RGD- and NGR-modified polymeric nanomedicines. *Nano Lett.* **14**, 972–981 (2014).

162. Weaver, J. L. *et al.* Evaluating the potential of gold, silver, and silica nanoparticles to saturate mononuclear phagocytic system tissues under repeat dosing conditions. *Part. Fibre Toxicol.* **14**, 25 (2017).

163. Liu, T., Choi, H., Zhou, R. & Chen, I. W. RES blockade: A strategy for boosting efficiency of nanoparticle drug. *Nano Today* **10**, 11–21 (2015).

164. germain, matthieu *et al.* Abstract 3613: Mononuclear phagocytic system occupancy to increase nanomedicines based treatment efficacy. in *Cancer Chemistry* **79**, 3613–3613 (American Association for Cancer Research, 2019).

165. Vollmar, B., Rüttinger, D., Wanner, G. A., Leiderer, R. & Menger, M. D. Modulation of kupffer cell activity by gadolinium chloride in endotoxemic rats. *Shock* **6**, 434—441 (1996).

166. Husztik, E., Lázár, G. & Párducz, A. Electron microscopic study of Kupffer-cell phagocytosis blockade induced by gadolinium chloride. *Br. J. Exp. Pathol.* **61**, 624–630 (1980).

167. Cai, P., Kaphalia, B. S. & Ansari, G. A. S. Methyl palmitate: Inhibitor of phagocytosis in primary rat Kupffer cells. *Toxicology* **210**, 197–204 (2005).

168. Wolfram, J. *et al.* A chloroquine-induced macrophage-preconditioning strategy for improved nanodelivery. *Sci. Rep.* **7**, 13738 (2017).

169. Diagaradjane, P., Deorukhkar, A., Gelovani, J. G., Maru, D. M. & Krishnan, S. Gadolinium Chloride Augments Tumor-Specific Imaging of Targeted Quantum Dots *In Vivo*. *ACS Nano* **4**, 4131–4141 (2010).

170. Van Rooijen, N. Liposomes for targeting of antigens and drugs: Immunoadjuvant activity and liposome-mediated depletion of macrophages. *J. Drug Target.* **16**, 529–534 (2008).

171. Rooijen, N. Van & Sanders, A. Liposome mediated depletion of macrophages: mechanism of action, preparation of liposomes and applications. *J. Immunol. Methods* **174**, 83–93 (1994).

172. Hao, J. *et al.* Temporary suppression the sequestrated function of host macrophages for better nanoparticles tumor delivery. *Drug Deliv.* **25**, 1289–1301 (2018).

173. Samuelsson, E., Shen, H., Blanco, E., Ferrari, M. & Wolfram, J. Contribution of Kupffer cells to liposome accumulation in the liver. *Colloids Surfaces B Biointerfaces* **158**, (2017).

174. Lehenkari, P. P. *et al.* Further insight into mechanism of action of clodronate: Inhibition of mitochondrial ADP/ATP translocase by a nonhydrolyzable, adenine-containing metabolite. *Mol. Pharmacol.* **61**, 1255–1262 (2002).

175. Ohara, Y. *et al.* Effective delivery of chemotherapeutic nanoparticles by depleting host Kupffer cells. *Int. J. Cancer* **131**, 2402–2410 (2012).

176. Hu, Q., Van Rooijen, N. & Liu, D. Effect of macrophage elimination using liposome-encapsulated dichloromethylene diphosphonate on tissue distribution of liposomes. *J. Liposome Res.* **6**, 681–698 (1996).

177. Kirby, A. C., Beattie, L., Maroof, A., Van Rooijen, N. & Kaye, P. M. SIGNR1-negative

red pulp macrophages protect against acute streptococcal sepsis after Leishmania donovani-induced loss of marginal zone macrophages. *Am. J. Pathol.* **175**, 1107–1115 (2009).

178. Wolfram, J. *et al.* A chloroquine-induced macrophage-preconditioning strategy for improved nanodelivery. *Sci. Rep.* **7**, 13738 (2017).

179. Li, Y. P. *et al.* PEGylated PLGA nanoparticles as protein carriers: Synthesis, preparation and biodistribution in rats. *J. Control. Release* **71**, 203–211 (2001).

180. Sun, X. *et al.* An assessment of the effects of shell cross-linked nanoparticle size, core composition, and surface PEGylation on in vivo biodistribution. *Biomacromolecules* **6**, 2541–2554 (2005).

181. Snehalatha, M., Venugopal, K., Saha, R. N., Babbar, A. K. & Sharma, R. K. Etoposide Loaded PLGA and PCL Nanoparticles II: Biodistribution and Pharmacokinetics after Radiolabeling with Tc-99m. *Drug Deliv.* **15**, 277–287 (2008).

182. Yang, L. *et al.* Size dependent biodistribution and toxicokinetics of iron oxide magnetic nanoparticles in mice. *Nanoscale* **7**, 625–636 (2015).

183. Reddy, L. H. & Murthy, R. S. R. *PHARMACOKINETICS AND BIODISTRIBUTION STUDIES OF DOXORUBICIN LOADED POLY(BUTYL CYANOACRYLATE) NANOPARTICLES SYNTHESIZED BY TWO DIFFERENT TECHNIQUES*.

184. Xie, G., Sun, J., ZhonG., G., Shi, L. & ZhanG., D. Biodistribution and toxicity of intravenously administered silica nanoparticles in mice. *Arch. Toxicol.* **84**, 183–190 (2010).

185. Meng, H. *et al.* Use of size and a copolymer design feature to improve the biodistribution and the enhanced permeability and retention effect of doxorubicin-loaded mesoporous silica nanoparticles in a murine xenograft tumor model. *ACS Nano* **5**, 4131–4144 (2011).

186. Meng, F., Wang, J., Ping, Q. & Yeo, Y. Quantitative Assessment of Nanoparticle Biodistribution by Fluorescence Imaging, Revisited. *ACS Nano* **12**, 6458–6468 (2018).

187. Rao, L. *et al.* Erythrocyte Membrane-Coated Upconversion Nanoparticles with Minimal Protein Adsorption for Enhanced Tumor Imaging. *ACS Appl. Mater. Interfaces* **9**, 2159–2168 (2017).

188. Sonavane, G., Tomoda, K. & Makino, K. Biodistribution of colloidal gold nanoparticles after intravenous administration: Effect of particle size. *Colloids Surfaces B Biointerfaces* **66**, 274–280 (2008).

189. Xiao, K. *et al.* The effect of surface charge on in vivo biodistribution of PEG-oligocholic acid based micellar nanoparticles. *Biomaterials* **32**, 3435–3446 (2011).

190. Lipka, J. *et al.* Biodistribution of PEG-modified gold nanoparticles following intratracheal instillation and intravenous injection. *Biomaterials* **31**, 6574–6581 (2010).

191. Cole, A. J., David, A. E., Wang, J., Galbán, C. J. & Yang, V. C. Magnetic brain tumor targeting and biodistribution of long-circulating PEG-modified, cross-linked starch-coated iron oxide nanoparticles. *Biomaterials* **32**, 6291–6301 (2011).

192. Morais, T. *et al.* Effect of surface coating on the biodistribution profile of gold nanoparticles in the rat. *Eur. J. Pharm. Biopharm.* **80**, 185–193 (2012).

193. Os, T. & Weber, W. Overcoming Physiological Barriers to Nanoparticle Delivery-Are We

There Yet? *Bioeng. Biotechnol* **7**, 415 (2019).

194. Sindhwani, S. *et al.* The entry of nanoparticles into solid tumours. *Nat. Mater.* 1–10 (2020). doi:10.1038/s41563-019-0566-2

195. O'Brien, M. E. R. *et al.* Reduced cardiotoxicity and comparable efficacy in a phase III trial of pegylated liposomal doxorubicin HCl (CAELYX^{TM}/Doxil®) versus conventional doxorubicin for first-line treatment of metastatic breast cancer. *Ann. Oncol.* **15**, 440–449 (2004).

196. Safra, T. *et al.* Pegylated liposomal doxorubicin (doxil): Reduced clinical cardiotoxicity in patients reaching or exceeding cumulative doses of 500 mg/m2. *Ann. Oncol.* **11**, 1029–1033 (2000).

197. Petersen, G. H., Alzghari, S. K., Chee, W., Sankari, S. S. & La-Beck, N. M. Meta-analysis of clinical and preclinical studies comparing the anticancer efficacy of liposomal versus conventional non-liposomal doxorubicin. *J. Control. Release* **232**, 255–264 (2016).

198. Lazarovits, J. *et al.* Supervised Learning and Mass Spectrometry Predicts the in Vivo Fate of Nanomaterials. *ACS Nano* **13**, 8023–8034 (2019).

199. Sharma, S. *et al.* Intravenous Immunomodulatory Nanoparticle Treatment for Traumatic Brain Injury. *Ann. Neurol.* **87**, 442–455 (2020).

200. Hanson, M. C. *et al.* Nanoparticulate STING agonists are potent lymph node-targeted vaccine adjuvants. *J. Clin. Invest.* **125**, 2532–2546 (2015).

201. Liu, H. *et al.* Structure-based programming of lymph-node targeting in molecular vaccines. *Nature* **507**, 519–522 (2014).

202. Irvine, D. J. & Dane, E. L. Enhancing cancer immunotherapy with nanomedicine. *Nature Reviews Immunology* 1–14 (2020). doi:10.1038/s41577-019-0269-6

203. Sato, Y., Kinami, Y., Hashiba, K. & Harashima, H. Different kinetics for the hepatic uptake of lipid nanoparticles between the apolipoprotein E/low density lipoprotein receptor and the N-acetyl-d-galactosamine/asialoglycoprotein receptor pathway. *J. Control. Release* (2020). doi:10.1016/j.jconrel.2020.03.006

204. Abraham, S. A. *et al.* The liposomal formulation of doxorubicin. *Methods Enzymol.* **391**, 71–97 (2005).

205. Epstein-Barash, H. *et al.* Physicochemical parameters affecting liposomal bisphosphonates bioactivity for restenosis therapy: Internalization, cell inhibition, activation of cytokines and complement, and mechanism of cell death. *J. Control. Release* **146**, 182–195 (2010).